KIT

Karlsruhe Institute of Technology

Two-Stage Stochastic Program Optimizing the Total Cost of Ownership of Electric Vehicles in Commercial Fleets

Maximilian Schücking, Patrick Jochem

No. 50 | NOVEMBER 2020

WORKING PAPER SERIES IN PRODUCTION AND ENERGY

Two-Stage Stochastic Program Optimizing the Total Cost of Ownership of Electric Vehicles in Commercial Fleets

Maximilian Schücking, Patrick Jochem

Chair of Business Administration, Production and Operations Management, Institute for Industrial Production (IIP), Karlsruhe Institute for Technology (KIT), Hertzstr. 16, 76187 Karlsruhe, Germany
Email: maximilian.schuecking@partner.kit.edu, jochem@kit.edu

The possibility of electric vehicles to technically replace internal combustion engine vehicles and to deliver economic benefits mainly depends on the battery and the charging infrastructure as well as on annual mileage (utilizing the lower variable costs of electric vehicles). Current studies on electric vehicles' total cost of ownership often neglect two important factors that influence the investment decision and operational costs: firstly, the trade-off between battery and charging capacity; secondly the uncertainty in energy consumption. This paper proposes a two-stage stochastic program that minimizes the total cost of ownership of a commercial electric vehicle under uncertain energy consumption and available charging times induced by mobility patterns and outside temperature. The optimization program is solved by sample average approximation based on mobility and temperature scenarios. A hidden Markov model is introduced to predict mobility demand scenarios. Three scenario reduction heuristics are applied to reduce computational effort while keeping a high-quality approximation. The proposed framework is tested in a case study of the home nursing service. The results show the large influence of the uncertain mobility patterns on the optimal solution. In the case study, the total cost of ownership can be reduced by up to 3.9% by including the trade-off between battery and charging capacity. The introduction of variable energy prices can lower energy costs by 31.6% but does not influence the investment decision in this case study. Overall, this study provides valuable insights for real applications to determine the techno-economic optimal electric vehicle and charging infrastructure configuration.

Two-Stage Stochastic Program Optimizing the Total Cost of Ownership of Electric Vehicles in Commercial Fleets

Maximilian Schücking [a]*, Patrick Jochem [a]

[a] Institute for Industrial Production (IIP), Karlsruhe Institute of Technology (KIT), Hertzstraße 16, D-76187 Karlsruhe, Germany
* Corresponding author: Phone +49 721 608 44590
E-mail addresses: maximilian.schuecking@partner.kit.edu, jochem@kit.edu

ABSTRACT

The possibility of electric vehicles to technically replace internal combustion engine vehicles and to deliver economic benefits mainly depends on the battery and the charging infrastructure as well as on annual mileage (utilizing the lower variable costs of electric vehicles). Current studies on electric vehicles' total cost of ownership often neglect two important factors that influence the investment decision and operational costs: firstly, the trade-off between battery and charging capacity; secondly the uncertainty in energy consumption. This paper proposes a two-stage stochastic program that minimizes the total cost of ownership of a commercial electric vehicle under uncertain energy consumption and available charging times induced by mobility patterns and outside temperature. The optimization program is solved by sample average approximation based on mobility and temperature scenarios. A hidden Markov model is introduced to predict mobility demand scenarios. Three scenario reduction heuristics are applied to reduce computational effort while keeping a high-quality approximation. The proposed framework is tested in a case study of the home nursing service. The results show the large influence of the uncertain mobility patterns on the optimal solution. In the case study, the total cost of ownership can be reduced by up to 3.9% by including the trade-off between battery and charging capacity. The introduction of variable energy prices can lower energy costs by 31.6% but does not influence the investment decision in this case study. Overall, this study provides valuable insights for real applications to determine the techno-economic optimal electric vehicle and charging infrastructure configuration.

Keywords:
Battery electric vehicle; Total cost of ownership; Stochastic programming; Hidden Markov model; Scenario reduction

1. Introduction

Almost a quarter of all greenhouse gas emissions in Europe are caused by transport, which is also the main contributor to local air pollution in cities [1]. These two negative impacts have become a dominating topic in public and political discussions. The introduction of electric vehicles (EVs) is propagated as one promising way to decrease local and global emissions from road transport [2,3]. However, the current market success of EVs is developing slowly.

Due to their characteristics, commercial applications have the potential to overcome the three main remaining techno-economic disadvantages of EVs in comparison to internal combustion engine vehicles (ICEVs). These are their limited range, the duration of recharging, and the higher purchase price. Research on commercial transport has shown that the range of current EV models is suitable for most tours and that lower variable costs for operation might outbalance the higher purchase prices of EVs [4,5]. Therefore, commercial transport, which results in higher annual mileage than privately owned vehicles, is considered a promising introductory market since it also has more predictable regular mobility patterns and faster turnover rates [4,6,7]. Its share in the registration of new

passenger cars is substantial; in Germany it amounts to approximately 65% [8].

Due to the limited range and duration of recharging, a detailed analysis of the underlying mobility patterns is required when assessing the substitution potential of EVs. Mobility patterns have a strong impact on energy consumption as well as on the timeslots available for charging. Hence, they have a strong effect on the investment decision concerning the required battery capacity and the charging capacity of the electric vehicle supply equipment (EVSE) as well as the operational costs. Next to the mobility patterns, the outside temperature can also significantly influence the actual energy consumption. Both are subject to uncertainties [9–11]. These sources of uncertainty should be considered in investment planning. Evaluating the influence of the mobility patterns requires detailed information on individual driving tours. However, for most commercial vehicle operations, only little information is available and data on complete driving patterns in high time resolutions are scares. To the best of the authors' knowledge, the existing literature lacks a comprehensive methodical framework for jointly optimizing the investment decision and operational costs of an EV while considering the empirical uncertainties of energy consumption and available charging times during operation based on limited time-series data.

This paper attempts to fill this gap by proposing a two-stage stochastic program in combination with a detailed technical EV model which ensures the full technical substitutability in the investment decision while minimizing the total cost of ownership (TCO) of the vehicle and charging infrastructure. The stochastic program is solved by sample average approximation (SAA). A hidden Markov model (HMM) is introduced to generate the required stochastic input parameters based on limited empirical time series data. To reduce computational effort while keeping a good approximation of the optimal value, a newly developed adaptation of an existing scenario reduction heuristic is proposed. This is tested in a case study of the home nursing service. With 13,300 providers, over 350,000 employees, and around 700,000 patients needing home care, it is an important and common use case in Germany [12].

1.1 Related work

In the literature, the optimization of the technical configuration and TCO of EVs in commercial fleets has been rarely addressed, so far. In the smart home context, several studies assessed the EV investment for private customers [e.g. 13,14]. Table 1 compares different studies that focus on commercial fleets. The generalized research focus of these studies is the competitiveness of different vehicle technologies based on fleet size and vehicle routing optimization. Hiermann et al. [15] specifically focus on the methodical advancements of these optimization approaches to include specific EV characteristics such as charging times.

All papers listed in Table 1 consider EV investment as part of the optimization, as can be seen in line 2. Most of them also evaluate the effect of different battery capacities (line 3). They do so either by comparing different available EV models [16,18] or by introducing a finite number of exemplary vehicles [15,17]. All of these papers consider battery capacity as an exogenous parameter and not an endogenous decision variable. Assumed that the previously deployed ICEVs are fully substituted, an exogenous given battery capacity may only lead by chance to a cost minimal EV investment choice or require the individual assessment of all possible parameter values. Furthermore, only Davis & Figliozzi [16] include battery aging in their analysis by evaluating different replacement scenarios (line 4). However, they do not consider battery aging in their model as a constraint that decreases the actually available battery capacity during utilization.

Most of the studies consider the vehicle and the required EVSE investment, as shown in line 5. They do so either indirectly by including costs for public charging [15] or directly through the investment of own charging or battery swapping stations [17–19]. As part of the investment decision, two papers compare fast charging and swapping stations (line 6). None of the studies compares the effect of variable charging capacities directly. Four papers consider the required charging time as can be seen in line 7. They do so in a simplified way by assuming a constant charging power and completed charging (i.e. a state of charge (SOC) of 100%) at the end of each charging process). However, partially recharging during empirical operations is often observed and might provide a significantly more economical solution. None of the studies investigate the optimization potential that focuses on the trade-off between the investment in battery and charging capacity (line 8).

	Davis & Figliozzi 2013 [16]	Hiermann et al. 2016 [15]	Kuppusamy et al. 2017 [17]	Lebeau et al. 2015 [18]	Sathaye 2014 [19]	Our contribution
(1) Commercial application	Delivery trucks	Delivery trucks	Taxi fleet	Delivery vehicles	Taxi fleet	Home nursing service
(2) EV investment	✓	✓	✓	✓	✓	✓
(3) Variable battery capacity	(✓)	(✓)	(✓)	(✓)		✓
(4) Battery aging model	(✓)					(✓)
(5) EVSE investment		(✓)	✓	✓	✓	✓
(6) Variable charging capacity			(✓)		(✓)	✓
(7) Flexible state of charge (SOC) model		(✓)	(✓)	(✓)	(✓)	✓
(8) Trade-off between investment in battery and charging capacity						✓
(9) Detailed energy consumption model	✓			✓		✓
(10) Empirical mobility patterns	(✓)			(✓)		✓
(11) Impact of uncertainty (mobility patterns & outside temperature)						✓

Table 1 Outline of previous research on configuration and cost optimization of EVs in commercial applications (ratings in brackets mean that the aspect is only considered to a limited extent)

Two papers consider detailed technical energy consumption for the EVs (line 9), but only rely on a limited empirical data base (line 10). The other papers assume constant consumption levels. Davis & Figliozzi [16] estimate the energy consumption based on driving cycles and a detailed vehicle dynamics model. Lebeau et al. [18] specifically expand the new methodical approach by Hiermann et al. [15] by an energy consumption model. The authors identify this as the central missing component. Therefore, they add a linear regression model based on the input data from one vehicle with trip duration and temperature as input variables. Even though research has shown that mobility patterns and outside temperature have a strong influence on energy consumption as well as available charging times and are subject to

uncertainty, none of the presented studies consider the impact of this uncertainty on the investment decision and operational costs in their model, as shown in line 11.

Solely focusing on the operation of EVs, the effect of uncertain mobility demand on the optimization potential is a commonly researched topic. [e.g. 20–23]. Since these studies focus on the utilization, the battery and charging capacity are set as exogenous parameters. This allows the use of dynamic programming or optimal control for optimization. These approaches cannot be applied when also considering the investment as part of the optimization. Kley [24] proposes a potential solution by incorporating the dynamic optimization into a TCO model for privately owned EVs. This study evaluates the TCO for different battery and charging capacity scenarios, which are again set as exogenous parameters. Jointly optimizing investment and cost of operations under uncertainty requires an alternate methodical approach.

Two-stage stochastic programs are commonly applied in the context of one-time investment decisions [25,26]. The method is based on the fundamental assumption that the decision itself has no influence on the sources of uncertainty [27]. SAA has been established as a standard way to approximate the expected cost function by a finitely discrete set of scenarios, that reflect the observed uncertainty [28,29]. The stochastic program is transformed into a deterministic equivalent with the scenarios representing possible realizations in the decision-making horizon. The complex nature of the underlying uncertainty distribution can require the inclusion of many scenarios. Here, scenario reduction, in which the original set of scenarios is approximated with a smaller representative subset, can be used to limit the computational burden while keeping a high quality of the solution [30]. This approach of a stochastic program with SAA and scenario reduction can be applied to jointly optimize the investment decision and operational costs while taking the uncertain energy consumption into account and without risking exaggerated computing times.

A subsequent methodical challenge lies in the generation of the required stochastic mobility patterns as input scenarios for the stochastic program. For the generation of stochastic driving patterns different temporal distributions, e.g. Weibull, Gamma, and log-normal distribution, are put forward and compared in the literature with inconclusive results [31–33]. Moreover, for vehicle dynamics, the Markov property has been validated [34] and Markov chains are applied to model driving cycles on empirical driving patterns [35,36]. However, using Markov chains for modeling driving patterns requires a fine temporal data resolution of speed and acceleration values. This information is rarely available in real-world commercial applications.

Hidden Markov models (HMMs) can be applied when only limited time-series information is available. Examples of application areas are natural phenomena [37,38], financial markets [39,40], or predictive maintenance [41,42]. An HMM is a white box method which has the advantage of a clear mathematical structure and has proved its value in modeling dynamic systems under uncertainty [43]. HMMs can outperform exponential, Weibull, log-normal, and exponential mixture models [38,44]. An HMM has been applied to model simple EV driving patterns by Iversen et al. [45]. To the authors' knowledge, this methodology has never been applied to model commercial driving tours.

1.2 Contributions and structure of this study
As illustrated in the literature review and Table 1, to the best of the authors' knowledge, there is a gap in the current literature: The body of literature lacks a comprehensive methodical framework for optimizing investment choice and operational costs when introducing EVs in

commercial applications that also considers detailed technical EV characteristics and the uncertain actual energy consumption and available charging times during operation.

The study at hand attempts to fill this gap by presenting a two-stage stochastic program, which allows optimizing both the investment decision (first-stage) and expected operational cost (second-stage) for commercial EVs under different sources of uncertainty. The investment decision includes the trade-off between battery and charging capacity. The stochastic program builds on a detailed technical EV model containing energy consumption, charging load-curves, and battery aging. Based on the literature, the mobility patterns and outside temperature are included as key sources of uncertainty for the actual energy consumption and available charging times. Amongst others, detailed information on mobility patterns is required as input to the technical EV model. However, based on their practical experience, the authors assume that only limited information on mobility patterns, e.g. from a logbook, is available in everyday commercial mobility applications. Therefore, an HMM is introduced as an approach for generating mobility scenarios. Furthermore, the paper presents a new scenario reduction heuristic to facilitate a more efficient approximation of the optimal TCO value. All things considered, several methodical approaches and small advancements are newly combined into a comprehensive TCO optimization framework.

This framework is applied to a home nursing service case study. Despite being a common mobility application, the home nursing service, as are other services, is rarely in the focus of transportation research [46,47].

In conclusion, the major contributions of this paper are:

1. Developing an overall investment and operations choice formula, which considers battery capacity, charging capacity, as well as uncertain energy consumption and available charging times under the constraints of a detailed technical EV model.
2. Predicting the stochastic mobility demand patterns based on limited empirical time-series data by training and using an HMM for scenario generation.
3. Comparing three scenario reduction heuristics, one of which is a newly developed advancement, to identify the one that most efficiently approximates the optimal value of the two-stage stochastic model.
4. Applying the newly developed approach to a home nursing service case study, which, despite being a common mobility application, has received little research attention.

The remainder of this paper is structured as follows: Section 2 proposes the two-stage stochastic TCO program, introduces the HMM used for scenario generation, and describes the three applied scenario reduction heuristics. Section 3 outlines the set-up of the case study. Section 4 presents the results as well as their discussion and critical appraisal. Section 5 concludes the paper with a summary and an outlook for future work.

2. Two-stage stochastic program with scenario generation

The techno-economic optimization of the EV investment and operation is based on a TCO approach. TCO goes beyond the initial price to understand the true cost of buying a particular good or service [48]. It is commonly used for EV assessment to ponder the higher purchase price against the savings in operational costs in comparison to ICEV. Implementing the framework provided by Götze and Weber [49] the target group of this study are commercial fleet operators and the techno-economic assessment follows a cost-based approach. In this study, only battery electric vehicles are considered. Fig. 1 provides an overview of the model and data input.
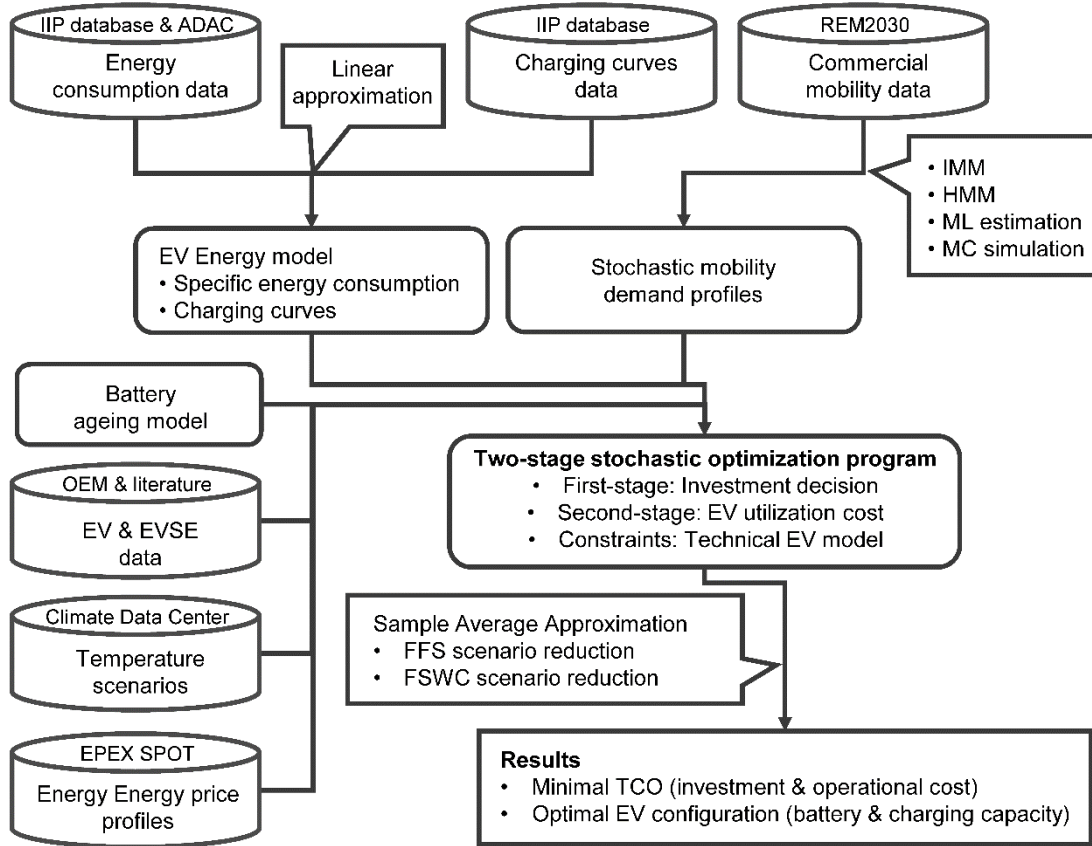
Fig. 1 Structural overview of the proposed techno-economic optimization model

2.1 Two-stage stochastic program

This paper proposes a two-stage stochastic program with multi-periodic costs to account for the uncertainty in the actual energy demand during the one-time investment decision. This approach allows optimizing the TCO by jointly minimizing the costs of the first-stage decision (investment in EV and EVSE) and the expected costs of the second-stage decisions (vehicle usage costs). The SAA method is applied to approximate the expected costs of the second-stage decisions. In the SAA method, a random finite sample of the stochastic input parameters is generated based on the underlying probability distribution. In the case at hand, this sample consists of mobility and temperature scenario sets. These scenarios are used to approximate the expected objective function value of the second-stage costs. For the probability of occurrence of the individual scenarios, a uniform probability distribution is assumed. As a result, the stochastic program is transformed into a deterministic equivalent specified by the sample. Applying deterministic optimization techniques can then solve the problem.

2.1.1 Objective function

Battery and charging capacity are set as the two key technical investment choices. When minimizing the TCO on condition that the mobility requirements will fully be met, the investments in battery and charging capacity form a trade-off. A large battery capacity enables many tours on one charge; a high charging capacity allows for faster recharges between the tours and hence, a smaller battery can be sufficient. The gross battery capacity $BCAP^G$ is set as the first-stage decision variable. For each of the charging capacity alternatives c, the model is solved individually to avoid quadratic constraints in the piecewise linear approximated flexible load curves. The second-stage decision variables charging

power $P^{crg}_{t,s^{mob},s^{temp}}$ and state of charge $SOC^{bat}_{t,s^{mob},s^{temp}}$ pertain to the charging decisions during operations in each period t under the realization of the scenarios for mobility demand s^{mob} and ambient temperature s^{temp}, which are considered stochastically independent.

Indices	
T	set of time periods in the planning horizon
A	set of years in the planning horizon
C	set of EVSE types distinguished by charging capacity
S^{mob}	set of mobility demand scenarios
S^{temp}	set of temperature scenarios

Deterministic parameters	
$INV^{EV}_{a_0 c}$	one-time EV and EVSE investment [€]
INV^V	EV net purchasing price without battery [€]
INV^{EVSE}_c	EVSE net purchasing price of charging station type c [€]
$INST^{EVSE}_c$	net installation cost of EVSE charging station type $c \in C$ [€]
$INV^{bat}_{a_0}$	net purchasing price battery [€]
pr^{bat}_a	specific net battery price on a system level in year $a \in A$ [€/kWh]
$RV^{EVSE}_{a,c}$	residual value of the EVSE in year $a \in A$ [€]
c^{batref}_a	net battery refurbishment cost in year $a \in A$ [€/kWh]
$f^{batSL}_{0.7}$	factor battery second-life value level of the current market price
$\alpha, \beta_1, \beta_2, \beta_3$	regression parameters of the residual value (α constant, β_1 age, β_2 monthly distance, β_3 purchase price)
i	interest rate
d	time resolution (duration of one period) [h]
A^{EVSEd}	EVSE depreciation time [a]
pr^{el}_t	electricity price in period $t \in T$ [€/kWh]
c^{EVma}	EV maintenance cost [€/km]
c^{EVtax}	EV annual tax [€]
c^{EVins}	EV annual insurance cost [€]
f^{EVSEma}	factor indicating the annual EVSE maintenance cost as a proportion of the purchase price
P^{maxcrg}_c	charging capacity of EVSE type $\in C$ [kW]
RP_c	remaining battery capacity that sets of charging capacity reduction of EVSE type $c \in C$ [kWh]
f^{EVgn}	factor battery net of gross capacity available for charging and discharging
η^{crg}	overall charging efficiency from the grid to battery
EC^{el}	EV specific energy consumption depending on $BCAP^G, DS^{spd}_{t,s^{mob}}$ and $Temp^{amb}_{t,s^{temp}}$ [kWh/km]
w^{batcap}	factor for warranted battery capacity at the end of the first-life
$w^{batdist}$	warranted distance before the end of the first-life [km]
$w^{battime}$	warranted time before the end of the first-life [a]
$\hat{p}_{jk}(t)$	maximum-likelihood estimator of the transition probabilities of the discrete inhomogeneous Markov model
$n_{jk}(t)$	number of historic observations for starting a tour at time $t \in T$
B	number of parameters in the hidden Markov model
H	number of hidden states in the hidden Markov model
O	number of observations in the hidden Markov model
L	log-likelihood of the training data for a specific hidden Markov model
q_m	number of key first-stage decision combinations in the FSWC heuristic
q	target number of scenarios in the FSWC heuristic
pr^{const}	net electricity wholesale price in the base case [€/kWh]
$pr^{EPEX\ SPOT}_{\varnothing,2014}$	annual average of the electricity wholesale price [€/kWh]
$pr^{EPEX\ SPOT}_{t,2014}$	hourly electricity wholesale price at time $t \in T$ [€/kWh]
M	number of scenarios generated by Monte-Carlo simulation
δ	risk level assessing Monte-Carlo simulation confidence
ε	accuracy of estimated mean from Monte-Carlo simulation results

$C^{op}(s^{mob}, s^{temp})$	total operational costs depending on the mobility s^{mob} and temperature scenario s^{temp} [€]
$RV_{a,c}^{EV}(s^{mob})$	total residual value of EV and EVSE in year $a \in A$ depending on the mobility scenario s^{mob} [€]
$RV_a^V(s^{mob})$	residual value of the vehicle without battery in year $a \in A$ depending on the mobility scenario s^{mob} [€]
$RV_a^{bat}(s^{mob})$	residual value of the battery in year $a \in A$ depending on the mobility scenario s^{mob} [€]
$DIST(s^{mob})$	total mileage traveled depending on the mobility scenario s^{mob} [km]
$w_a^{ucap}(s^{mob})$	battery state of health in year $a \in A$ depending on the mobility scenario s^{mob}
$C^{EVEN}(s^{mob}, s^{temp})$	energy cost depending on the mobility s^{mob} and temperature scenario s^{temp} [€]
$C^{EVMA}(s^{mob})$	EV maintenance cost depending on the mobility scenario s^{mob} [€]
C^{EVTI}	fixed annual costs for insurance and taxes [€]
C^{EVSEMA}	fixed annual for EVSE maintenance [€]
$EC^{el}\left(DS_{t,s^{mob}}^{spd}, \mathrm{BCAP}^G, Temp_{t,s^{temp}}^{amb}\right)$	electric energy consumption depending on driving speed $DS_{t,s^{mob}}^{spd}$, battery capacity BCAP^G and outside temperature $Temp_{t,s^{temp}}^{amb}$ [kWh/km]
$o_{kj}^{[1]} := o(\omega_k, \omega_j)$	Kantorovich distance between the second-stage costs of two scenarios k and j used for scenario selection in the FSWC_O heuristic

$DS_{t,s^{mob}}^{crg}$	EV charging state in mobility scenario $s^{mob} \in S^{mob}$ in period $t \in T$
$DS_{t,s^{mob}}^{drv}$	EV driving state in mobility scenario $s^{mob} \in S^{mob}$ in period $t \in T$
$DS_{t,s^{mob}}^{spd}$	EV average speed in mobility scenario $s^{mob} \in S^{mob}$ in period $t \in T$
$p_{s^{mob}}$	probability that scenario s^{mob} occurs
$Temp_{t,s^{temp}}^{amb}$	ambient temperature in temperature scenario $s^{temp} \in S^{temp}$ in period $t \in T$ [°C]
$p_{s^{temp}}$	probability that scenario s^{temp} occurs

$BCAP^G$	first-stage variable representing the gross battery capacity of the EV, integer [kWh]
$P_{t,s^{mob},s^{temp}}^{crg}$	second-stage variable representing the charging power in period $t \in T$ under the mobility scenario $s^{mob} \in S^{mob}$ and temperature scenario $s^{temp} \in S^{temp}$, continuous [kW]
$SOC_{t,s^{mob},s^{temp}}^{bat}$	second-stage variable representing the state of charge (SOC) in period $t \in T$ under the mobility scenario $s^{mob} \in S^{mob}$ and temperature scenario $s^{temp} \in S^{temp}$, continuous [kWh]

Table 2 Nomenclature

The objective function represents the TCO with the investment $INV_{a_0 c}^{EV}$, as well as the expected operational costs $C^{op}(s^{mob}, s^{temp})$, and residual value $RV_{a,c}^{EV}(s^{mob})$. By applying SAA, the objective function is written as sum of the investment, as first-stage decision, and the expected second-stage costs as the calculated average of all scenarios.

$$\min_{c \in C} INV_{a_0 c}^{EV} + \sum_{s^{mob} \in S^{mob}, s^{temp} \in S^{temp}} p_{s^{mob}} \, p_{s^{temp}} \left(C^{op}(s^{mob}, s^{temp}) - RV_{a,c}^{EV}(s^{mob}) \right) \qquad (1)$$

For the one-time investment, the net purchase prices for the vehicle (without the battery) INV^V, the battery $INV_{a_0}^{bat}$, the EVSE INV_c^{EVSE}, and the net costs for installation $INST_c^{EVSE}$ are considered.

$$INV_{a_0 c}^{EV} = INV^V + INV_{a_0}^{bat} + INV_c^{EVSE} + INST_c^{EVSE} \qquad (2)$$

The price of the vehicle INV^V is set fixed. The battery price $INV_{a_0}^{bat}$ depends on the market price for battery capacity on system level $pr_{a_0}^{bat}$ in the year the investment is made.

$$INV_{a_0}^{bat} = pr_{a_0}^{bat} BCAP^G \tag{3}$$

The investment and installation costs of the EVSE $INST_c^{EVSE}$ are fixed and depend on the selected type c.

The EV and EVSE in this analysis are sold at the end of the planning horizon. Hence, their residual values must also be taken into account.

$$RV_{a,c}^{EV}(s^{mob}) = RV_a^V(s^{mob}) + RV_a^{bat}(s^{mob}) + RV_{a,c}^{EVSE} \tag{4}$$

The residual values of the vehicle and the battery depend on the intensity of use over time and therefore the respective mobility scenario s^{mob}. The intensity of use is represented by the total mileage traveled $DIST(s^{mob})$ which itself depends on the mobility demand $DS_{t,s^{mob}}^{spd}$ in the respective scenario s^{mob} and the time resolution d.

$$DIST(s^{mob}) = \sum_{t \in T} DS_{t,s^{mob}}^{spd} \, d \tag{5}$$

The calculation of the vehicle's residual value $RV_a^V(s^{mob})$ is based on the linear regression formula developed by Linz, Dexheimer, & Kathe [50] also applied for EVs in Plötz et al. [6] where readers are referred to for detailed information concerning the model.

$$RV_a^V(s^{mob}) = \frac{e^\alpha e^{\beta_1 12a} e^{\frac{\beta_2}{12} \frac{DIST(s^{mob})}{a_{end}}} INV^{V\beta_3}}{(1+i)^a} \tag{6}$$

The residual value of the battery $RV_a^{bat}(s^{mob})$ is estimated based on the battery ageing in terms of the remaining capacity in year a.

$$RV_a^{bat}(s^{mob}) = \frac{\left[\left(\left(\frac{f_{0.7}^{batSL} - w^{batcap}}{1 - w^{batcap}}\right) + \left(\frac{1 - f_{0.7}^{batSL}}{1 - w^{batcap}}\right) w^{ucap}(s^{mob})\right) pr_a^{bat} - c_a^{batref}\right] BCAP^G}{(1+i)^a} \tag{7}$$

Fischhaber, Regett, Schuster, & Hesse [51] have developed a model in which the residual value of the battery $RV_a^{bat}(s^{mob})$ in year a depends on the state of health (SOH) $w_a^{ucap}(s^{mob})$ and its second-life use-value. At the end of the first life w^{batcap} the resale value after refurbishment c_a^{batref} lies only at a factor $f_{0.7}^{batSL}$ of the current price for a new battery system.

This study takes a practical approach towards battery aging to limit the complexity and avoid non-linear constraints. Empirical studies show that for C-rates[1] of 1 c or less, which can be expected as the outcome of the presented model, the capacity fade is close to linear [52,53]. The warranties provided by the manufacturers are taken as references to model the worst-case linear decline. The warranties of the manufacturers usually guarantee utilization, e.g. 150,000 km, and durability, e.g. 8 years. To account for both limitations, the battery degradation factor in this study $w^{ucap}(s^{mob})$ is calculated as the minimum two terms: First, the total mileage in the mobility scenario in relation to the maximum warranted distance; second, the investment period in relation to the warranted durability.

$$w_a^{ucap}(s^{mob}) = min\left\{\frac{w^{batdist} - \left(DIST(s^{mob})\right)}{w^{batdist}}, \frac{w^{battime} - a_{end}}{w^{battime}}\right\} \tag{8}$$

---

[1] The C-rate stands for the ratio of the applied (dis-)charging current to the capacity of the battery, e.g. for a battery a capacity of 40 Ah a charging current of 80 A means a C-rate of 2.

For residual values of EVSE type c in year a, $RV_{a,c}^{EVSE}$ there are currently no well-founded models. Therefore, following the legal depreciation time a linear loss of value independent of the intensity of use is assumed.

$$RV_{c,a}^{EVSE} = \frac{INV_{c,a_0}^{EVSE}\left(1-\frac{a}{A^{EVSEd}}\right)}{(1+i)^a} \tag{9}$$

The costs of operation are divided into fixed and variable costs with the variable costs $C^{EVEN}(s^{mob}, s^{temp})$ and $C^{EVMA}(s^{mob})$ depending on the assumed mobility demand s^{mob} and ambient temperature s^{temp} scenario.

$$C^{op}(s^{mob}, s^{temp}) = C^{EVEN}(s^{mob}, s^{temp}) + C^{EVMA}(s^{mob}) + C^{EVTI} + C^{EVSEMA} \tag{10}$$

Fixed are the annual costs for insurance and taxes

$$C^{EVTI} = \sum_{a\in A} \frac{c^{EVtax} + c^{EVins}}{(1+i)^a} \tag{11}$$

as well as EVSE maintenance for each year a of operation.

$$C^{EVSEMA} = \sum_{a\in A} \frac{INV_c^{EVSE} f^{EVSEma}}{(1+i)^a} \tag{12}$$

The energy and EV maintenance costs are variable. The energy costs depend on the total energy charged during operation, the electricity price pr_t^{el} in period t, and the chosen time resolution d.

$$C^{EVEN}(s^{mob}, s^{temp}) = \sum_{t\in T} P_{t,s^{mob},s^{temp}}^{crg} pr_t^{el} d \tag{13}$$

EV maintenance costs are set variable only depending on the distance traveled $DIST(s^{mob})$ in the specific mobility demand scenario s^{mob}.

$$C^{EVMA}(s^{mob}) = DIST(s^{mob}) c^{EVma} \tag{14}$$

2.1.2 Constraints

The technical model of the EV sets the constraints for the stochastic program. In the following, the focus lies on the energy model. The non-linear progressions of the energy consumption and charging curves are piecewise linearly approximated (see Section 5.1 and Appendix C). This approach leads to higher quality results than the commonly assumed fixed maximum capacity while the overall problem remains linear [54]. The thermal behavior of the battery is neglected.

The mobility scenarios determine when the EV can be charged. No public charging is included as risk mitigation. Currently, only limited public charging stations are available. Therefore, in the opinion of the authors, commercial applications, in which mobility is an essential part of the service, should not be dependent on the accessibility of public charging stations. Hence, the vehicle is only available for charging when parking on company grounds (the binary charging parameter $DS_{t,s^{mob}}^{crg} = 1$ and the binary driving parameter $DS_{t,s^{mob}}^{drv} = 0$).

$$P_{t,s^{mob},s^{temp}}^{crg} = 0, \ \forall \ t \in T, s^{mob} \in S^{mob}, s^{temp} \in S^{temp} | DS_{t,s^{mob}}^{crg} = 0 \tag{15}$$

Four typically used AC charging types distinguished by their charging capacity are compared in this paper: Mode 2 with 2.2 kW from a domestic socket, Mode 3 with 3.7, 11, and 22 kW (IEC61851-1). The battery charging curve is piecewise approximated by two linear parts. Exemplary recorded curves can be found in Schücking et al. [55] or Landau et al. [56]. Starting from an empty battery a constant maximum power P_c^{maxcrg} can be utilized.

$$P^{crg}_{t,s^{mob},s^{temp}} \leq P^{maxcrg}_c, \forall\, t \in T, s^{mob} \in S^{mob}, s^{temp} \in S^{temp} \tag{16}$$

After reaching a certain threshold, in this study defined by the remaining battery capacity to charge, the charging capacity is reduced depending on the SOC $SOC^{bat}_{t,s^{mob},s^{temp}}$.

$$P^{crg}_{t,s^{mob},s^{temp}} \leq SOC^{bat}_{t,s^{mob},s^{temp}} \left(-\frac{P^{maxcrg}_c}{RP_c} \right) + \frac{w^{ucap}(s^{mob}) f^{EVgn} BCAP^G P^{maxcrg}_c}{RP_c}, \forall\, t \in T, s^{mob} \in$$
$$S^{mob}, s^{temp} \in S^{temp} \tag{17}$$

The reduction depends on the SOH $w^{ucap}(s^{mob})$ and the available net capacity f^{EVgn}. The point of reduction RP_c varies between the different types of EVSE. In this study, no vehicle-to-grid services such as providing energy back to the grid or other ancillary services are included (Appendix C1).

In the energy model, it is important to distinguish the different measurement points for assessing energy consumption. From the technical point of view the tank-to-wheel (TTW) energy consumption is relevant. From an economic point of view, the grid-to-wheel efficiency (GTW) must be considered. The losses due to transformation and resistances that occur between the grid and the battery are included in the charging efficiency factor η^{crg} [57].

The discrete energy model is set by the SOC in period $t+1$ which equals the SOC in period t plus the energy charged minus the energy consumed through driving calculated by the average speed $DS^{spd}_{t,s^{mob}}$ and the specific TTW energy consumption EC^{el} (Appendix C2).

$$SOC^{bat}_{t+1,s^{mob},s^{temp}} = SOC^{bat}_{t,s^{mob},s^{temp}} + \left[\left(P^{crg}_{t,s^{mob},s^{temp}} \eta^{crg} \right) - DS^{spd}_{t,s^{mob}} EC^{el} \left(DS^{spd}_{t,s^{mob}}, BCAP^G, Temp^{amb}_{t,s^{temp}} \right) \right] d$$
$$\forall\, t \in T, s^{mob} \in S^{mob}, s^{temp} \in S^{temp} \tag{18}$$

For the TTW energy consumption EC^{el} the average speed $DS^{spd}_{t,s^{mob}}$ (drag), the additional battery weight (rolling resistance) and the ambient temperatures $Temp^{amb}_{t,s^{temp}}$ (auxiliary load) are considered as individual influence factors. The SOC can never exceed the maximum available capacity

$$SOC^{bat}_{t,s^{mob},s^{temp}} \leq w^{ucap}(s^{mob}) f^{GN} BCAP^G, \forall\, t \in T, s^{mob} \in S^{mob}, s^{temp} \in S^{temp} \tag{19}$$

and must always be positive.

$$SOC^{bat}_{t,s^{mob},s^{temp}} \geq 0\ \forall\, t \in T, \forall s^{mob} \in S^{mob}, s^{temp} \in S^{temp} \tag{20}$$

Furthermore, the SOC level after purchase (period t_0) and when the EV is sold at the end of the time (period t_{end}) are set to be the same.

$$SOC^{bat}_{t_0,s^{mob},s^{temp}} = SOC^{bat}_{t_{end},s^{mob},s^{temp}}, \forall s^{mob} \in S^{mob}, s^{temp} \in S^{temp} \tag{21}$$

2.2 Scenario generation with a hidden Markov model

The mobility demand scenarios are one core input to the SAA. They consist of different tours taken by the EV over a fixed period. A tour starts with leaving the company grounds and ends with the return. It can consist of several trips and intermediate stops, which makes it a complex structure to predict. The key parameters required by the optimization model are the starting time of the tour as well as the parameters of the individual trips and stops during the tour.

The stochastic model used to generate the scenarios from the historical data and forecast the future mobility demand consists of three parts: an inhomogeneous Markov model to predict the starting point of the tours, a multinomial HMM to generate the individual tours, and a set of conditional normal distributions to estimate the mean speed per trip depending on the duration.

Since the probability of starting a tour is dependent on the time of day in line with previous studies, a discrete inhomogeneous Markov model is used to account for the temporal variance of the transition probabilities [45]. The maximum-likelihood estimator of the transition probabilities $\hat{p}_{jk}(t)$ for visible states S, can be calculated based on the historic observations $n_{jk}(t)$ at time t.

$$\hat{p}_{jk}(t) = \frac{n_{jk}(t)}{\sum_{l=1}^{N} n_{jl}(t)} \, , \forall \, j, k \in S \tag{22}$$

HMMs are finite mixture models. They consist of two parts: an unobserved parameter process and an observed state-dependent process (Appendix A). The unobserved parameter process satisfies the Markov property and can, therefore, be applied to driving cycle modulation. HMMs can be trained on historical data in supervised learning. The most common approach to find the estimates of the model parameters is the Baum-Welch algorithm [58]. This paper applies a strategy version for this algorithm based on Biernacki, Celeux, & Govaert [59] with several runs and different random starting parameters (Appendix A). This approach does not guarantee a global optimum but reduces the risk of getting stuck in a local one [60].

Different evaluation criteria are used to identify the best suitable HMM. The number of hidden states cannot be deduced from the data. An ex-post evaluation is necessary. With each additional hidden state, the model fit indicated by the log-likelihood increases. However, so does the number of parameters. In the case of the multinomial-HMM, the number of parameters B is calculated by $B = H + H^2 + H \cdot O$ where H is the number of hidden states and O is the number of observations. To avoid an overcomplex model two commonly used evaluation metrics are applied. The Akaike information criterion (AIC) [61]

$$AIC = -2 \log L + 2B \tag{23}$$

and the Bayes information criterion (BIC) [62].

$$BIC = -2 \log L + B \log O \tag{24}$$

Both provide relative model quality estimates, where L is the log-likelihood of the training data. The HMM with the lowest values is the best fitting model.

As an additional selection criterion k-fold cross-validation is used. It is a standard practice in supervised statistical learning to ensure out-of-sample predictive performance [63]. k-fold cross-validation is applicable to HMMs [64]. In this paper, 4-fold cross-validation is chosen. In each run ¾ of data are taken for training while ¼ is left out for testing.

The last part of the stochastic driving profile generation is the estimation of each trip's mean speed. For driving profiles, the mean speed increases with the total driving distance of the trip [65]. Accordingly, speed and trip duration cannot be considered independent. For different intervals of duration, separate normal distributions are assumed based on the historical data with the statistical value as maximum likelihood estimators for μ and σ.

2.3 Scenario reduction heuristics

The complex nature of the underlying uncertainty distribution often requires many scenarios for the SAA. Since the approximated deterministic model is solved considering all scenarios simultaneously, this can lead to a significant computational burden. The most common approach to limiting the computational burden while keeping a high quality of the solution is to approximate the original set of scenarios with a smaller representative subset. Fast forward selection (FFS) is a commonly applied scenario reduction heuristic that relies on the probability metrics of the stochastic input parameters when generating the representative subset [30,66].

Over the years, FFS has faced some criticism for its sole focus on the input parameters and their failure to consider the individual scenario's impacts on the first-stage decision and second-stage cost. The literature proposes different advancements that build on FFS but cluster the scenarios according to key first-stage decision variables or consider the individual scenario's impact on the optimum value [67–69].

Adding to this line of research, three different scenario reduction heuristics are compared in the following: FFS heuristic (Appendix B) introduced by Heitsch & Römisch [30] as well as two versions of forward selection in wait-and-see-clusters (FSWC) heuristic proposed by Feng & Ryan [67].

The FSWC heuristic differs from FFS by including the key first-stage decision variables in the scenario reduction process by implementing the following four steps:
- Step 1:
  For each mobility scenario, the deterministic subprogram is solved, and the key first-stage decision variables are recorded.
- Step 2:
  The scenarios are clustered by their first-stage decision variables. If the number of first-stage decision variable combinations q_m is equal to or smaller than the target number of scenarios q step 3 can be skipped.
- Step 3:
  The number of groups q_m is reduced by clustering them into q clusters. Instead of the k-means clustering algorithm [70] used by Feng & Ryan [67] the improved k-means++ [71] method is applied in this paper to create the clusters q.
- Step 4:
  For each of the clusters, one representative scenario is selected by using FFS. The probabilities of the unselected scenarios in the cluster are added to the probability of the selected one.

In the presented framework the battery and charging capacity are used for clustering.

As an additional approach, this paper proposes a new advancement of the original FSWC algorithm (in the following called FSWC_S). The new version (in the following called FSWC_O), also considers the overall output performance of the individual scenarios. In step 4, instead of selecting the representative scenario for each cluster based on the Kantorovich distance between their probability distributions, the second-stage costs of the individual optimization runs are used, represented by $o_{kj}^{[1]} \coloneqq o(\omega_k, \omega_j)$. The required information is already available through the individual solution of the deterministic subprograms from step 1. Therefore, no additional effort is required in comparison to FSWC_S. The motivation behind this advancement is to provide a potentially more efficient way of approximating the optimum value of the presented two-stage stochastic model. This

can be achieved by having even smaller scenario subsets delivering a high-quality solution and therefore reducing the computational time of the overall program.

3. Data and case study design

The stochastic program is implemented for the home nursing service use case: Nurses drive around in small vehicles to attend to care-dependent people in their homes. Its technical and organizational requirements can be met by the properties of EVs. Mobility is essential to the operations and the mobility cost is the second-highest cost item after labor. The fleets usually consist of EVs from the mini or small segment. The tours show a high frequency of starts and stops with an annual mileage of 15,000 km in urban and 20,000 km in rural environments. Due to the frequent short trips, combustion engines are especially inefficient leading to high fuel consumption and maintenance costs. Previous research has identified it as one of the most promising commercial use cases for early EV introduction [4,5].

Technical and financial EV and EVSE properties, electricity prices, mobility demand, and temperature are the data input to the model. Whenever possible literature values are validated with current market information or directly taken from manufacturers or leasing companies (Table 3). Also, direct data from operations, e.g. charging infrastructure maintenance, electricity prices, insurance, and warranties are used.

The estimation of the specific energy consumption in dependence of the mean speed per trip is split into three components: the energy consumed by propulsion, the additional energy consumption due to the battery weight, and the energy required by the auxiliaries depending on the outside temperature (Appendix C1). The resulting, here piecewise linearly approximated, specific energy consumption curve in Fig. 2 shows the distinctive progression that can also be found in empirical studies [e.g. 72–74].
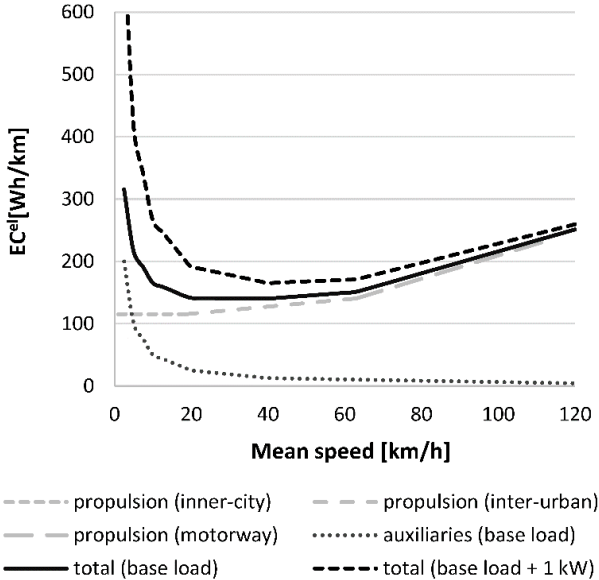
Fig. 2 Linear approximation of the EV specific energy consumption depending on the average speed and auxiliary demand (Appendix C1, Source: ADAC)

Parameter	Value	Explanation & source
a_0	2017	year of investment
INV^V	20,000 €	the mean EV net purchase price with basic configuration and no battery (mini and small car segment) [75]
pr^{bat}_{2017}	210 €/kWh	the net battery price on a system level, mean value from the literature [76,77]; validated with current EV purchase prices [78]
pr^{bat}_{2020}	185 €/kWh	the net battery price on a system level, mean value from the literature [76,77]
$f^{batSL}_{0.7}$	0.5	the reselling price of the battery at the end of life will be around 50% of the current market price for a new comparable battery [51]
c^{batref}_a	50 €/kWh	estimation of the battery refurbishment cost based on the mean value from review by [51] assumed to be independent of a
α	0,97948	a constant from the regression model by [50]
β_1	$-1.437 \cdot 10^{-2}$	the age factor from the regression model by [50]
β_2	$-1.17 \cdot 10^{-4}$	the mileage factor from the regression model by [50]
β_3	0.91569	the purchase price factor from the regression model by [50]
a_{end}	3 a	assumption of EV usage time due to fast technological advances, 3.8 years is the current average for commercial vehicles [6]
d	1 min	time resolution of the model
i	5.02%	the mean value of interest rates in Germany over the last 10 years [79]
T^{EVSEd}	8 a	assumption based on comparable technical equipment, no reliable empirical data available or legal amortization period defined in Germany
pr^{el}_t	0.20 €/kWh	net price for electricity (assumed constant, since this is currently the case for most home nursing service providers in Germany) (EPEX SPOT)
c^{EVma}	0.024 €/km	the mean value of EV maintenance costs from the literature [80–82]
c^{EVtax}	0 €/a	EV are exempted from taxes and tolls in Germany
c^{EVins}	450 €	assumption for EV insurance based on interviews (IIP database)
f^{EVSEma}	0.10	assumption for EVSE maintenynce based on interviews with installation companies (IIP database)
f^{EVgn}	0.87	the mean current value for the gross to net battery capacity ratio estimated based on information provided by manufacturers of current EV models
η^{crg}	0.85	the mean value of charging efficiency based on own measurements and review [56,57]
w^{batcap}	0.70	the mean current value of warrantied battery capacity communicated by the manufactures of current EV models
$w^{batdist}$	160,000 km	the mean current value of warrantied battery lifetime milieage communicated by the manufactures of current EV models
$w^{battime}$	8 a	the mean current value of warrantied battery life communicated by the manufactures of current EV models
ρ^{bat}	95 Wh/kg	the energy density of current Li-ion batteries [81]
c_{rr}	0.0088	the rolling resistance coefficient mean value for tires on the road surface [81]
g	9.81 N/kg	the gravitational constant

Table 3 Overview of the technical and economic input parameters for the case study

Table 4 provides an overview of the four EVSE alternatives that are compared in this study. The progression of the piecewise linear charging load-curves can be seen in Fig. 3 (Appendix C2). The net purchase prices INV^{EVSE}_c for the EVSE are current mean market values. For the 2.2 kW, investment and installation costs are assumed to be zero since it only requires a separately protected standard power socket.

P_c^{maxcrg}	2.2 kW	3.7 kW	11 kW	22 kW
RP_c	1 kWh	1 kWh	3.5 kWh	7 kWh
INV_c^{EVSE}	0 €	600 €	1,200 €	1,800 €
$INST_c^{EVSE}$	0 €	100 €	200 €	300 €

Table 4 Technical and economic input parameters for the different EVSE alternatives (Sources: IIP database)
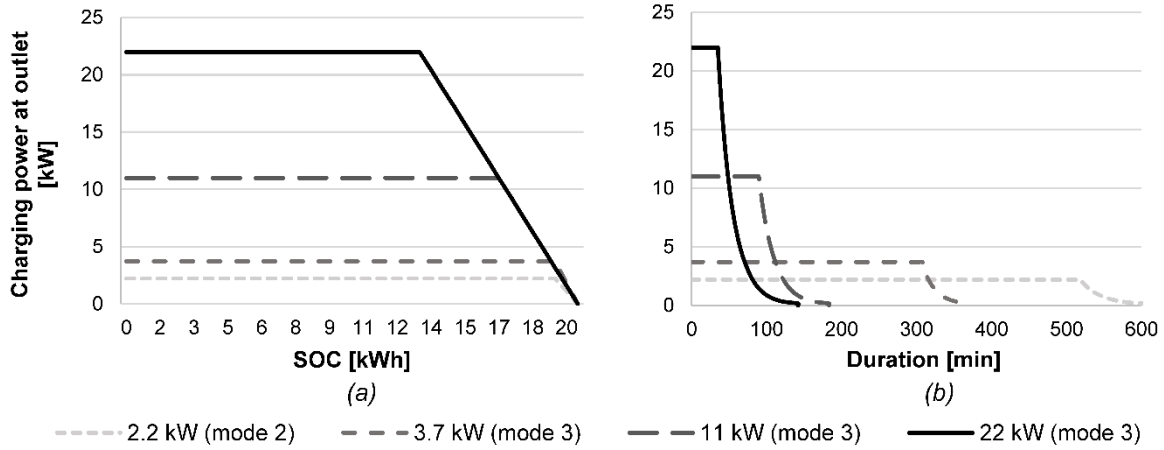
Fig. 3 Maximum available charging power for the EVSE alternatives depending on SOC (a) and duration (b) (Appendix C2, Source: IIP database)

The data input to train the mobility demand model is taken from the regional eco mobility 2030 (REM2030) project [83]. The empirical data consists of 91,422 single trips from 630 commercial ICEVs that were deployed by various companies from different economic segments over an average period of three weeks. For each trip the time of departure, arrival, the distance traveled, and the distance to the company are recorded. Also, metadata concerning the vehicles and companies is available [83]. This case study is based on ICEV data under the assumption that the mobility profiles will not change when EVs are introduced since they are determined by the customer and user demand.
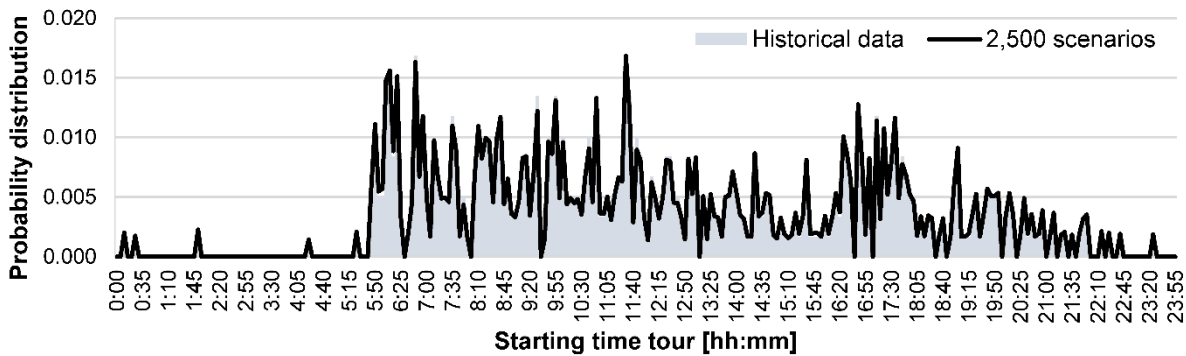
Fig. 4 Distribution of the tour starting times for the home nursing service case study (Source: REM2030 [83])

For this case study, one home nursing service company with ten vehicles and 1,698 logged trips is selected. The minimum of recorded trips per vehicle is 17 and the maximum 299. The demand for home-nursing service is independent of the weekday. The relative frequency of starting tours shows three high peaks throughout the day, indicating that in the morning, around noon, and in the late afternoon, there is a higher probability for starting a tour (Fig. 4).

16

The proposed model requires tours consisting of one or more cohesive, individual trips as input. Therefore, it is necessary to cluster the single recorded trips into tours that start and end at the company. The tours are created based on assumptions about the driving profiles. Unfortunately, the times at the company are not given in the data set. As a workaround, it is assumed that the vehicle has returned to the company if the waiting time between two trips is larger than 30 minutes. This approach has been approved by operators. Based on this approach 594 tour profiles are created. Since around 70% of all of the trips are shorter than 10 minutes with over 25% being shorter than 5 minutes a time resolution d of one minute is required to allow a detailed energy consumption assessment.

Temperature data for five large German cities from 1981 to 2016 provided by the Climate Data Center (CDC) is taken as data input for the temperature scenarios [84]. From readings at these five measurement points over 25 years, an average year with 52 weeks and hourly values is calculated as the set of temperature scenarios.

To analyze the effect of variable electricity prices on the battery and charging capacity investment decision as well as on the operational costs, flexible tariffs are introduced. In the base case, the net price for electricity pr_t^{el} is assumed to be constant. For the flexible tariffs, hourly electricity prices for Germany from 2014 at the European Power Exchange (EPEX SPOT) are taken and separated into 52 weekly scenarios. To assess the sensitivity of the optimal results to a flexible tariff, the weeks with the minimal, median, and maximal variation are selected (Table 5). The EPEX SPOT lists wholesale prices. Hence, additional charges must be considered. The final net price pr_t^{el} is calculated by subtracting the annual average wholesale price $pr_{\emptyset,2014}^{EPEX\,SPOT}$ from the net price in the base case pr_t^{const} and adding the hourly wholesale price $pr_{t,2014}^{EPEX\,SPOT}$.

$$pr_t^{el} = pr_t^{const} - pr_{\emptyset,2014}^{EPEX\,SPOT} + pr_{t,2014}^{EPEX\,SPOT} \tag{26}$$

Scenario	Mean pr_t^{el}	Minimum pr_t^{el}	Maximum pr_t^{el}
Constant	0.200 €/kWh	0.200 €/kWh	0.200 €/kWh
Flexible minimum	0.181 €/kWh	0.201 €/kWh	0.222 €/kWh
Flexible median	0.173 €/kWh	0.203 €/kWh	0.248 €/kWh
Flexible maximum	0.136 €/kWh	0.187 €/kWh	0.218 €/kWh

Table 5 Overview of the assessed electricity price scenarios (Source: EEX)

4. Case Study Results
The following section presents and discusses the results regarding the applied framework and implications for commercial applications.

4.1 Mobility scenario generation
As input to the framework, the empirical tour profiles are coded with the three introduced parameters $DS_{t,s^{mob}}^{crg}$, $DS_{t,s^{mob}}^{drv}$, and $DS_{t,s^{mob}}^{spd}$ which indicate the current status of the EV at any given point in time (Table 6).

Vehicle status	$DS_{t,s^{mob}}^{crg}$	$DS_{t,s^{mob}}^{drv}$	$DS_{t,s^{mob}}^{spd}$
EV is parked on company grounds and can be charged	1	0	0
EV is parked during a tour and cannot be charged	0	0	0
EV is driving	0	1	>0

Table 6 Overview of the three different vehicle states that are used to model the mobility scenarios

HMMs with different numbers of hidden states are trained to identify the best fitting model with the tour profiles assumed to be independent of the time of day. Four separate training and evaluation sets were created from the 594 empirical tours. The model training was implemented in Python using the *Annaconda* environment and the *hmmlearn* package with the functions *fit* to train the model, *score* to calculate the likelihood, and *predict* to decode the hidden states using the Viterbi algorithm. The training was run on a Win Server 2016 (x64) system with a 2x Intel Xeon 5430, 2.66GHz CPU, and 24 GB 4 Core RAM.

Hidden states	2	3	4	5	6	7	8
Score	-10,166.78	-9,833.68	-9,769.73	-9,735.75	-9,723.50	-9,722.33	-9,717.96
AIC	20,353.56	19,703.35	19,595.45	19,551.51	19,554.99	19,584.65	19,611.91
BIC	20,435.84	19,851.44	19,825.81	19,880.59	19,999.25	20.160.55	20,335.90
4-fold score	-2,759.53	-2,497.78	-2,486.18	-2,463.14	-2,467.39	-2,460.60	-2,460.56

Table 7 Model evaluation results for the HMMs with an increasing number of hidden states
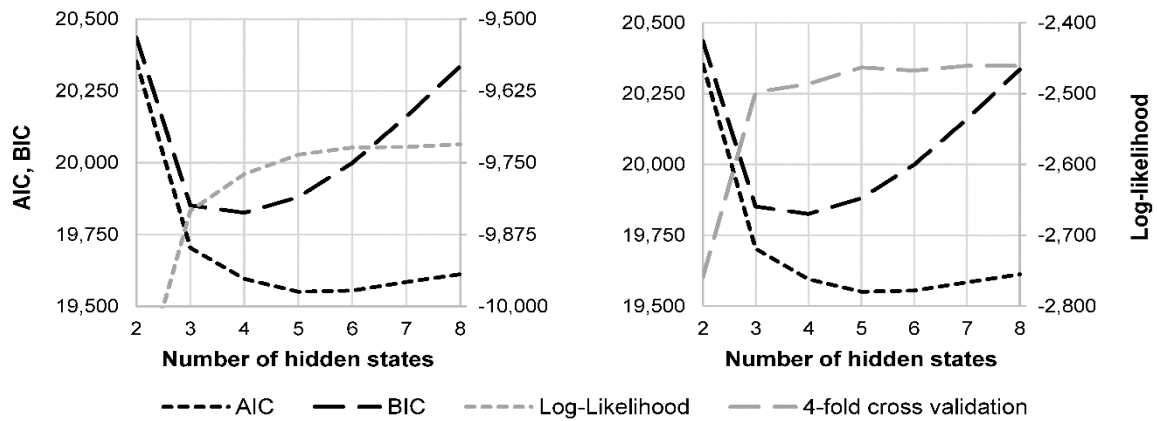
Fig. 5 AIC, BIC, log-likelihood, 4-fold cross-validation values of the HMMs with an increasing number of hidden states

The results of the model evaluation indicate that an HMM with either four or five hidden states has the best fit (Table 7 & Fig. 5). The BIC favors four hidden states, the AIC five. The 4-fold cross-validation as an indication for out-of-sample performance also favors the HMM with five hidden states. Further, increasing the number of hidden states delivers no significant gain in predictability (Table 7 & Fig. 5). Hence, the HMM with five hidden states is selected (Appendix B). The comparison of the empirical data and the scenarios created underlines the quality of the model (Fig. 4 & Fig. 6).
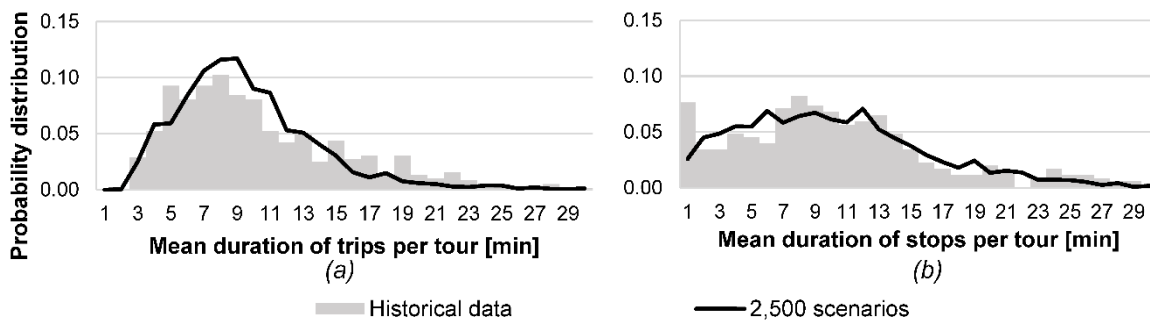
Fig. 6 Comparison of the historical data and the scenarios generated by the HMM

For estimation of the mean speed values in dependence of the individual trip duration, the empiric values are separated into five classes. For each class, a normal distribution is

assumed based on the ML estimation of μ and σ (Table 8). The goodness of fit is assessed with the Kolmogorov-Smirnoff (KS) test.

With the stochastic model, 2,500 scenarios of one-week mobility demand in one-minute time resolution were generated by Monte-Carlo simulation. The high number of scenarios M is required to ensure with 95% confidence (risk level δ = 0.05) that the estimated mean varies 5% (accuracy ε) or less from the original values for the four tour characteristics: number of trips per tour, mean duration of trips per tour, number of stops per tour, and mean duration of stops [85].

$$M \geq \Phi^{-1}(1-\delta)^2 \frac{\sigma^2}{\varepsilon^2} \tag{27}$$

	0-5 min	6-10 min	11-15 min	16-20 min	>20 min
μ	14.91	22.36	35.56	41.91	50.72
σ	8.42	11.04	13.95	13.34	15.58
KS test					
$\sqrt{r}L_n^{norm}$	$\sqrt{63}L_n^{norm}$ $= 0.57$	$\sqrt{205}L_n^{norm}$ $= 0.81$	$\sqrt{198}L_n^{norm}$ $= 0.68$	$\sqrt{63}L_n^{norm}$ $= 0.57$	$\sqrt{63}L_n^{norm}$ $= 0.67$
$l_{n;\,0,95}^{norm}$	$l_{>30;\,0,95}^{norm}$ $= 0.89$	$l_{>30;\,0,95}^{norm}$ $= 0.89$	$l_{>30;\,0,95}^{norm}$ $= 0.89$	$l_{>30;\,0,95}^{norm}$ $= 0.89$	$l_{>30;\,0,95}^{norm}$ $= 0.89$
Normal distribution	Cannot be rejected	Cannot be rejected	Cannot be rejected	Cannot be rejected	Cannot be rejected

Table 8 Results of the ML estimation for the normal distribution parameters of the average speed depending on trip duration and goodness of fit assessment

4.2 Subsets for scenario reduction

All scenario reduction algorithms were implemented in Python and run on a Win Server 2016 (x64) system with a 2x Intel Xeon 5430, 2.66GHz CPU, and 24 GB 4 Core RAM. Scenario subsets containing from 5 to 25 scenarios are created with each heuristic. In step 2 of the FSWC, the 2,500 individual sub-problem solutions can be clustered into 70 different combinations of optimal battery and charging capacity. Fig. 7 provides an overview of the relative frequency of the battery and charging capacity combinations as well as examples of clusters created out of the 70 combinations by the k-means++ algorithm in step 3.
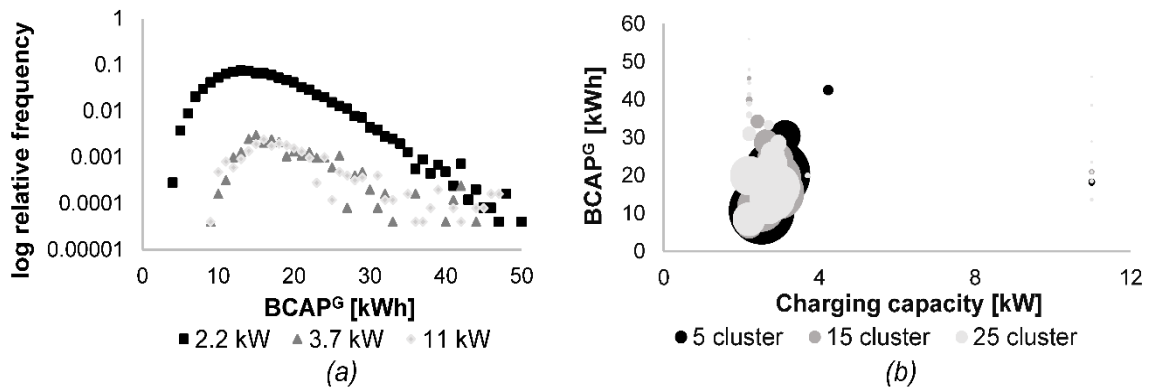
Fig. 7 Solutions of the individually optimized subprograms (a) and exemplary clusters created by the k-means++ algorithm (b)

4.3 Optimization

The optimization model is solved for scenario subsets of different sizes whose composition is determined by the three reduction heuristics. The program sizes for the different subsets can be found in Table 9. The optimization is implemented in Python 3.63, solved with the Gurobi solver (7.5.2), and run on a Win Server 2016 (x64) system with a 2x Intel Xeon 5430, 2.66GHz CPU, and 24 GB 4 Core RAM.

S^{mob}	No. of lines	No. of columns	No. of non-zeros	No. of continuous variables	No. of integer variables
5	3,528,002	1,512,014	5,608,024	1,512,013	1
10	7,056,002	3,024,014	11,208,684	3,024,013	1
15	10,584,002	4,536,014	16,937,014	4,536,013	1
20	14,112,002	6,048,014	22,739,234	6,048,013	1
25	17,640,002	7,560,014	28,520,874	7,560,013	1

Table 9 *Program size dependent on the number of mobility demand scenarios ($S^{temp} = 10$)*

4.3.1 Scenario reduction – mobility scenarios

The progression of the optimal value shows distinctive differences between the scenario reduction approaches. The optimal value is highly sensitive to the composition of scenarios selected. In comparison, both FSWC approaches require fewer scenarios than FFS to reach a stable approximated solution in the observed range (Fig. 8a). Furthermore, the stabilization level of the optimal value differs for all three algorithms. For smaller subsets, the optimal choice of charging capacities varies. From subsets containing 15 selected by FSWC and 20 by FFS onwards, 11 kW becomes the consistent cost-minimal choice. Detailed numerical results for all charging capacity alternatives can be found in Appendix D1.

The effects of increasing scenario subset sizes on the optimal gross battery capacity choice also shows distinctive differences between the three scenario reduction heuristics (Fig. 8b). With FFS the battery capacity increase is monotone. In each step, new mobility scenarios are added with some increasing the required optimal battery capacity. For scenario subsets selected by FSWC, the progress of the optimal battery and charging capacity configuration is more volatile. As new clusters are formed in each step, the composition of the most representative scenarios does not build on the selection in the smaller subsets. Like the optimal value and charging capacity, the optimal choice for battery capacity stabilizes with larger subset sizes. A small difference of 1 kWh remains between the optimal choice based on FSWC and FFS (Table D.1). This small discrepancy cannot explain the observed gap between the optimal TCO values generated by the three heuristics.
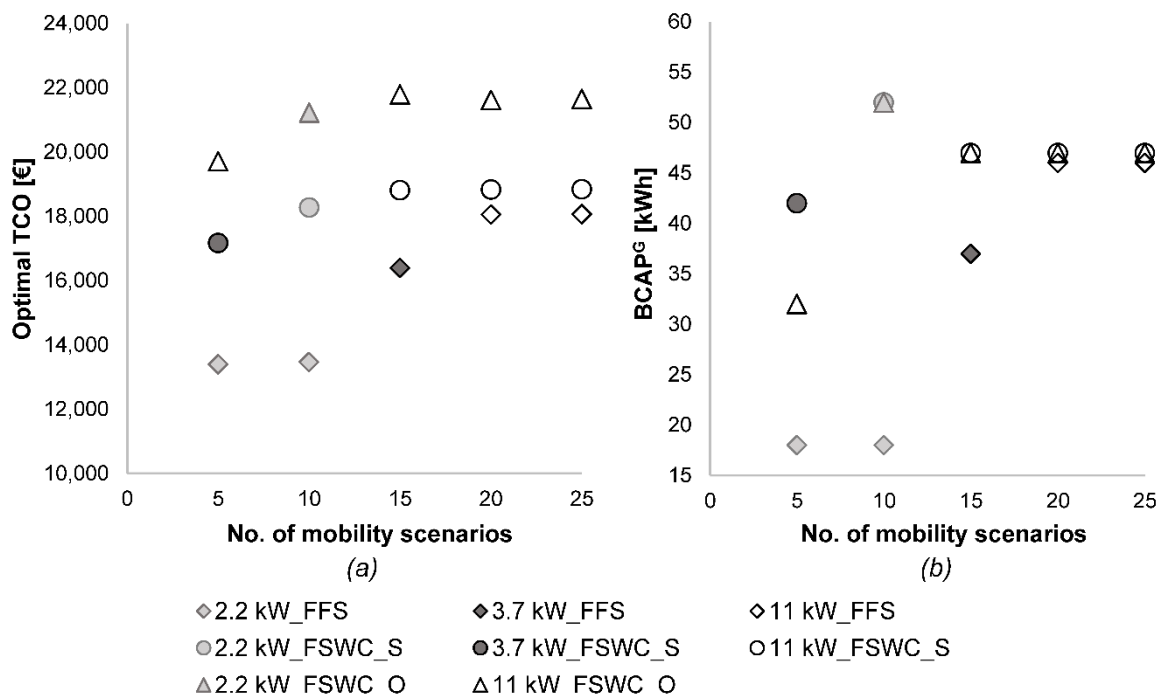
Fig. 8 *Optimal TCO values (a) and gross battery capacities (b) with an increasing number of mobility demand scenarios for the three reduction heuristics FFS, FSWC_S & FSWC_O ($S^{temp} = 10$)*
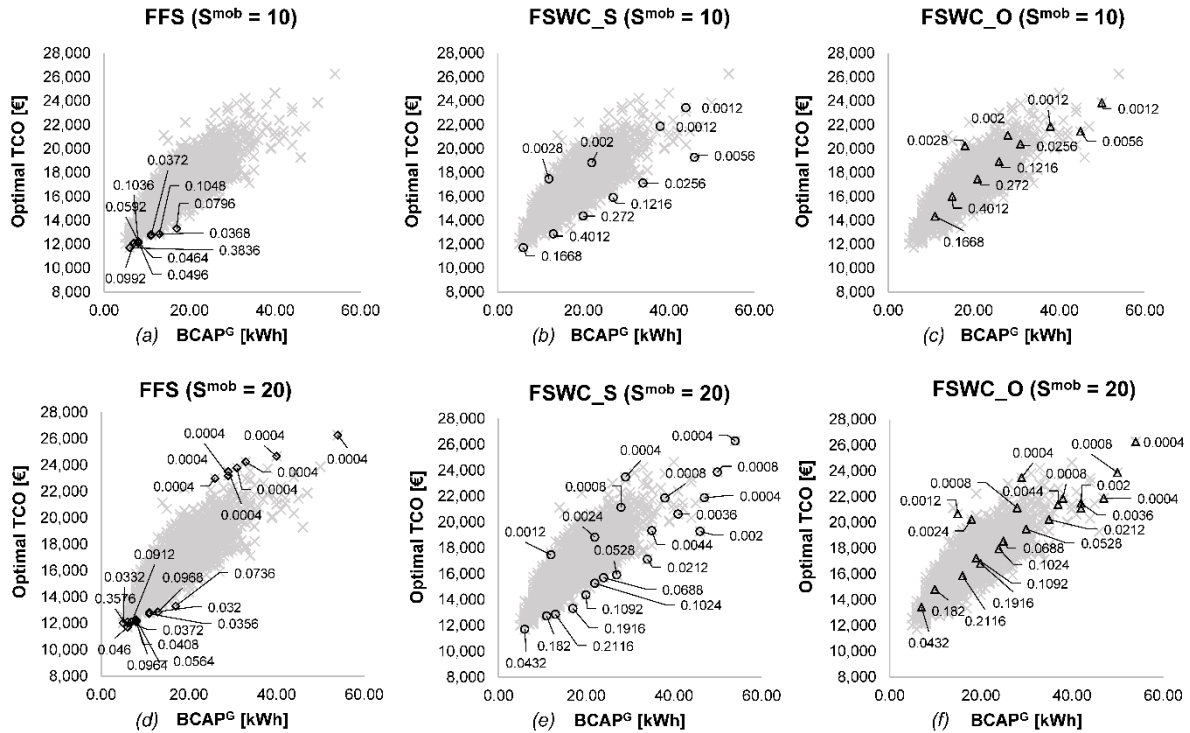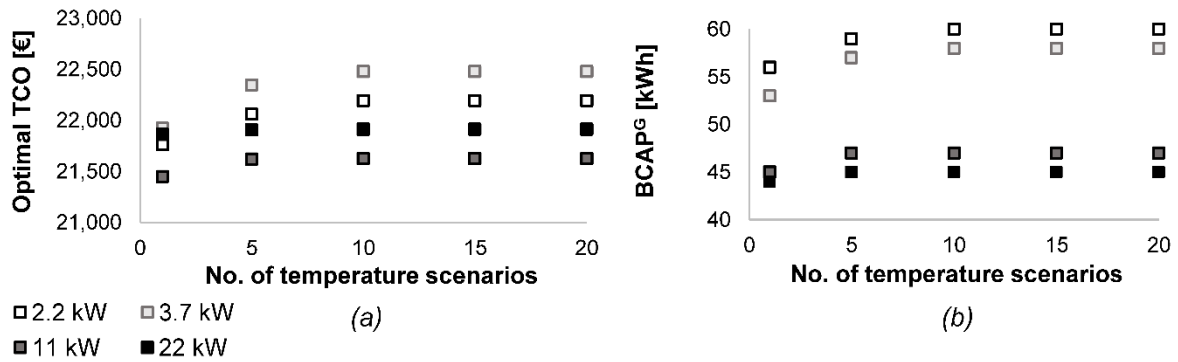
Fig. 9 Distribution of the optimal TCO values and battery capacity choices for the 2,500 individual subproblem solutions with the allocated probabilities compared for all three scenario reduction heuristics (S^{mob} = 10 or 20; S^{temp} = 10)

As is illustrated by Fig. 9, the gap can be explained by the second-stage cost distribution of the selected scenarios and their allocated probabilities. For the subset consisting of ten scenarios, FFS only selects scenarios that require a comparably low battery capacity. The optimal TCO values of the selected scenarios are at the lower boundary of the possible optimal TCO values for these configurations. In the subset of 20, also scenarios with individual solutions that have a large optimal battery capacity and comparatively high TCO values are included. However, they show rather low probabilities (0.0004). The scenario selection through FSWC_S and FSWC_O shows a more even distribution, but also distinctive differences (Fig. 9). The effect of selecting the representative scenario for each cluster and attributing the probabilities based on the second-stage costs as a measure for output performance, as it is done in the FSWC_O approach, becomes clearly visible.

4.3.2 Scenario reduction – temperature scenarios

The effect on the optimal TCO value and battery capacity for an increasing number of temperature scenarios differs notably from the mobility scenarios. The comparison of the subsets with an increasing number of scenarios selected by the FFS algorithm shows a fairly stable progression (Fig. 10). The charging capacity of 11 kW is always the cost-minimal choice. The optimal TCO value rises only slightly with the inclusion of more temperature scenarios. The outside temperature has only a small effect on the gross battery capacity, which rises from 45 to 47 kWh for the optimal TCO solution. Numerical results for the individual charging capacity alternatives can be found in Appendix D2.

Fig. 10 *Optimal TCO values (a) and gross battery capacity (b) with an increasing number of temperature scenarios (FFS, S^{mob} = 15)*

4.3.3 Evaluation of the stochastic approach and the applied heuristics

The comparison of the optimal TCO values resulting from the different scenario reduction heuristics shows that the newly proposed FSWC_O delivers the best approximation for our case study. The relative error to the solution for all 2,500 scenarios ($z_{2500}{}^*$) is 1.3% (Table 10). Hence, this solution is taken for the evaluation of the stochastic approach based on the expected value of perfect information (EVPI). The EVPI is calculated by the difference of the expected value of all individual subproblem solutions (EX_{2500}) and the optimal stochastic solution ($z_S{}^{mob*}$). It represents the amount one would be willing to pay for perfect foresight [25]. In this case study, the EVPI is 4,956 € (Table 10). The proportionally high value is owed to the large influence of the uncertain mobility patterns on the optimal investment decision. This underlines the importance of considering the uncertain energy demand in the investment decision even for the relatively regular mobility patterns of the home nursing service. The effect will arguably be even stronger for commercial use cases that show a higher variance in their mobility patterns.

	FFS	FSWC_S	FSWC_O
S^{mob}	25	25	25
$z_S{}^{mob*}$	18,071 €	18,847 €	21,656 €
P_c^{maxcrg}	11 kW	11 kW	11 kW
$BCAP^G$	46 kWh	47 kWh	47 kWh
$z_{2500}{}^*$	21,382 €	21,382 €	21,382 €
error	18.3%	13.5%	1.3%
EX_{2500}	16,700 €	16,700 €	16,700 €
EVPI			4,956 €

Table 10 *Overview of the solution quality for the different scenario reduction heuristics and the EVPI*

Due to the different process steps required for the applied scenario reduction heuristics, a clear statement concerning their computational efficiency is challenging. Taking only the final optimization into account, FSWC_O delivers the relatively best approximation. For a detailed comparison of the upstream process steps and potential benefit of parallelized subproblem optimization, the reader is referred to Feng & Ryan [67]. However, the results of the case-study show a clear advantage of the newly proposed FSWC_O compared to the FSWC_S. For both heuristics, the upstream process steps require the same computational time and resources. The second-stage costs taken for the selection of the most representative scenario in FSWC_O are already calculated for the individual subproblems in FSWC_S. Since the quality of the approximated solution is significantly higher for the same subset

sizes, in this case study FSWC_O outperforms FSWC_S (Table 10). A qualitative advantage of both FSWC versions over FFS is the transparency throughout the reduction process through the inclusion of the key first-stage decisions. Especially in the context of real applications, this can be an advantage.

4.4 Technological and economic implications for commercial mobility applications

The results of the case study provide interesting insights for commercial fleet operators to determine the techno-economic optimal EV and EVSE system configuration and TCO under uncertain energy consumption. The evaluation of the stochastic approach points to the importance of considering the uncertainty in the investment decision through joint optimization of the investment and expected operational costs. Based on the optimal choice of a gross battery capacity of 47 kWh and charging capacity of 11 kW, home nursing service fleet operators can scan the market to identify small EV models, with a suitable endowment. For example, the current version of the Renault ZOE Z.E. 50 with a gross battery capacity of 52 kWh and up to 22 kW charging capacity would meet the identified requirements.

The potential total cost savings enabled by the inclusion of the battery and charging capacity trade-off in the evaluation framework are notable (Table D.1). For FSWC_O (s^{mob} = 25, s^{temp} = 10) the optimal 11 kW solution reduces the TCO in comparison to the optimal 22 kW configuration by 1.3% (286 €). The cost advantage in comparison to the optimal 2.2 kW and 3.7 kW configurations are 2.6% (566 €) and 3.9% (852 €) respectively (Table D.1). When excluding the cost items, that are independent of the investment choice, e.g. the loss of value for the EV excluding the battery (Eq. 6), the proportional cost advantage increases to 3.2%, 6.3%, and 9.4% respectively. Hence, the results support the argumentation to consider different battery and charging capacity configurations in the investment decision.

The utilization of variable electricity prices combined with an optimal charging scheduling bears the potential for further TCO reductions. As can be seen in Fig. 11, charging EVs in low-price periods can reduce the second-stage cost through load shifting into periods with lower electricity prices. For the optimal 11 kW solution, the total energy costs over the investment period are 2,213 €. Under the assumption that the maximal volatile electricity price scenario would occur daily throughout the investment period, these costs could be reduced by 696 € (i.e. by 31.6%). Even though these effects are relatively small in relation to the overall TCO, variable electricity prices could also influence the optimal investment decision. However, in this case study, the introduction of flexible tariffs does not influence the optimal configuration of 47 kWh battery and 11 kW charging capacity in any of the assumed scenarios (Fig. 11). For other mobility applications, a faster charging option or a larger battery capacity allowing to use low-price periods more efficiently might influence the optimal trade-off between battery and charging capacity.
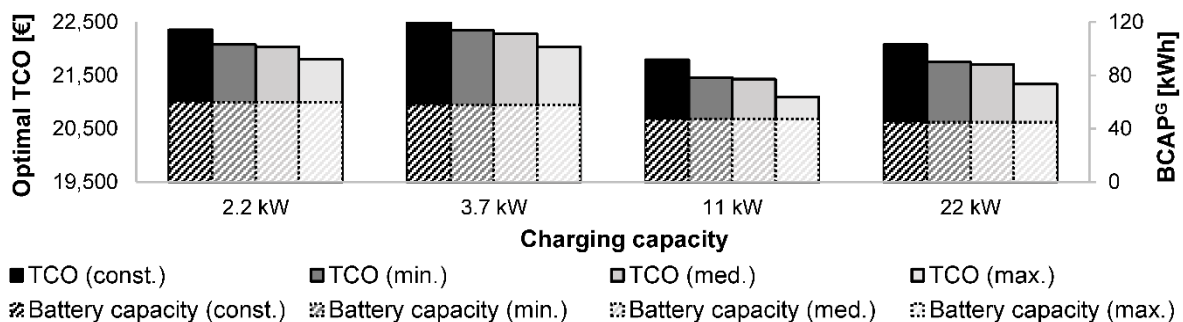

Fig. 11 *Optimal values and battery capacities for the different electricity price scenarios (FSWC_O, S^{mob} = 25; S^{temp} = 10)*

A detailed look into the upstream process steps of the FSWC heuristic provides additional insights that can potentially be beneficial in the investment decision. For the home nursing service case study only few mobility scenarios require battery capacities over 30 kWh or an 11 kW EVSE, when solved individually (Fig. 7 & Fig. 9). This is also reflected in the probabilities allocated to the selected scenarios (Table D.3). All scenarios, which when solved individually, require a battery capacity of less than or equal to 30 kWh, have a cumulative probability of 0.9576; all scenarios, which when solved individually, have a cost-minimal charging capacity of 11 kW, have a cumulative probability of only 0.0076. Hence, the transparency gained through the individual subproblem solution and scenario clustering helps to identify outlier scenarios. This may lead to a reconsideration of a full technical substitution as a condition for the introduction of EVs. In this case study, the willingness to exclude a small proportion of the mobility demand might lead to a system configuration with a significantly lower TCO.

Besides commercial fleet operators, the proposed framework may also be helpful for other user groups. For example, manufacturers of EV and EVSE can use it to draw conclusions on which vehicle configurations are required by commercial customers. Also, policymakers can apply the framework to evaluate the techno-economic substitution potential of EVs in widespread commercial applications. With the commercial vehicle market being an important introductory market, targeted subsidies for the identified mobility applications could notably accelerate the market introduction of EVs.

4.5 Critical appraisal

The suggested optimization approach and presented results are subject to various limitations that require consideration. Some limitations result from the lack of data. Also, simplifications are made to reduce the model complexity. For the overall framework, the key assumptions are that the vehicle must be able to fully cover all tours and the EV has its dedicated EVSE. As the basis for further optimization, both assumptions could be removed when considering a mixed commercial fleet. The abstraction of unrestricted battery capacity is chosen to identify the ideal configuration as a decision-making base for the investment. Currently, manufacturers offer two or three battery capacity choices for their current vehicle models, at best. Furthermore, the study neglects other sources of uncertainty that can influence energy consumption, e.g. the individual driving behavior, as well as the TCO, e.g. the development of electricity or battery prices. For the technical EV model, the key simplifications are the piecewise linear approximations of energy consumption, charging curves, and battery aging. Finally, based on this study, no general statements can be made about the criteria for selecting the appropriate scenario reduction heuristic. FFS worked well for the temperature scenarios; FSWC worked significantly better for the mobility scenarios. A possible explanation for this discrepancy might be the chosen modulation of the driving states based on the three parameters (Table 6). Overall, it can be stated that for the mobility scenarios in this case study, a similarity between two scenarios in the input distribution does not correlate to a similarity in the output of the model, i.e. optimal investment choice and second-stage costs. Hence, relying on the output performance instead of on the stochastic input parameters for scenario selection delivers a better approximation.

5. Conclusion and future work

This paper proposes a comprehensive methodical framework for optimizing the investment choice and operational costs when introducing electric vehicles in commercial fleets. It considers detailed technical electric vehicle characteristics and the uncertain actual energy

consumption and available charging times during operation. A two-stage stochastic program that minimizes the costs of the first stage (investment decision) and the second stage (vehicle usage costs) builds the core of the framework. The proposed approach specifically focuses on the trade-off between the electric vehicle's battery and charging capacity in the investment decision as well as on the influence that mobility demand patterns and outside temperature have on energy consumption and available charging times. The stochastic program is solved by sample average approximation. The mobility demand patterns, as part of the stochastic input parameters, are generated by a multinomial-hidden Markov model based on limited empirical time series data. To reduce the computational effort while keeping a good approximation, a newly developed adaptation of an existing scenario reduction heuristic is proposed. The overall framework is applied to a home nursing service case study.

The results of the case study show that the proposed framework is a well-suited approach to address the identified gap in the literature. The results illustrate the impact that mobility patterns and outside temperature as sources of uncertainty can have on the investment decision and therefore underline the importance of the stochastic approach. In the case study, allowing different battery and charging capacities in the investment decision can reduce the total cost of ownership. The influence of the mobility patterns on the investment decision is notably higher than the one of the outside temperatures. In the presented case, the introduction of variable electricity prices does not influence the optimal investment decision. Nevertheless, variable prices can lead to a lower total cost of ownership by enabling load-shifting into low price periods. Regarding the methodology applied, the newly proposed scenario reduction heuristic improves the quality of the approximated solution by including the overall output performance in the selection process with no additional computation effort. Additionally, the scenario clustering based on the optimal investment decision for their individual subproblems increases the transparency and provides valuable insights that can be beneficial in the investment decision. Moreover, the case study demonstrates that a hidden Markov model is well suited to generate stochastic commercial mobility patterns based on limited empirical time series data. In its entirety, the case analysis validates that the proposed framework can directly be applied by commercial fleet operators to determine the optimal electric vehicle and charging station configuration required for the substitution of an internal engine combustion vehicle and to minimize the related total cost of ownership.

Future work is needed to address the shortcomings of the presented framework and related open issues. The precision of the optimization model could be improved by considering the non-linearity of the technical constraints. Also, the hidden Markov model could be extended into an inhomogeneous model. Especially for use cases, where the tours differ in their characteristics throughout the day and between weekdays, an inhomogeneous approach would increase the predictability. Furthermore, the model could be applied to other mobility use cases to assess their potential and the suitability of the model. Also, additional sources of uncertainty could be included. Finally, future research could extend the optimization focus. One obvious extension would be to combine the model with a fleet size and routing optimization approach. This would make it possible to further optimize costs by utilizing the flexibility of different electric vehicle and charging infrastructure configurations or sharing common charging infrastructure between electric vehicles.

Funding Source

Appendix A
Hidden Markov model

Hidden Markov models (HMMs) are finite mixture models. They consist of two parts: an unobserved parameter process and an observed state-dependent process. The unobserved parameter process satisfies the Markov property.

$$Pr\left(Z_t|\mathbf{Z}^{(t-1)}\right) = \Pr(Z_t|Z_{t-1}), \forall t \in T \tag{A.1}$$

It can only be observed through the state-dependent process $\{X_t: t \in 1,2,\dots\}$ which is solely dependent on the current hidden state Z_t.

$$Pr\left(X_t|\mathbf{X}^{(t-1)}, \mathbf{Z}^{(t)}\right) = \Pr(X_t|Z_t), \forall t \in T \tag{A.2}$$

In contrast to independent mixture models, there is a temporal dependency. The current hidden state Z_t and therefore the state-dependent process hinges on the previous state Z_{t-1}.

$$p_i(x) = \Pr(X_t = x|Z_t = i) \; \forall t \in T \tag{A.3}$$

$p_i(x)$ is the probability mass function of X_t when the HMM is in a hidden state i at time t. In line with Zucchini et al. [44] three additional properties of the HMM are assumed: temporal homogeneity, stationarity of the Markov chain, and conditional independence. A multinomial HMM can be defined by (A, B, π): A is the matrix of the transmission probabilities between the hidden states, B is the matrix of state emission probabilities, and π is the vector of the initial state distribution.

The Baum-Welch algorithm used for training the HMM is a specific form of the EM algorithm which is generally applicable to finite mixture models [86] and makes use of the conditional independence assumption [39]. The likelihood of the estimated parameters increases monotone with every iteration. Depending on the initial parameters the progress can be slow, and it is never clear whether a local or a global optimum has been reached.
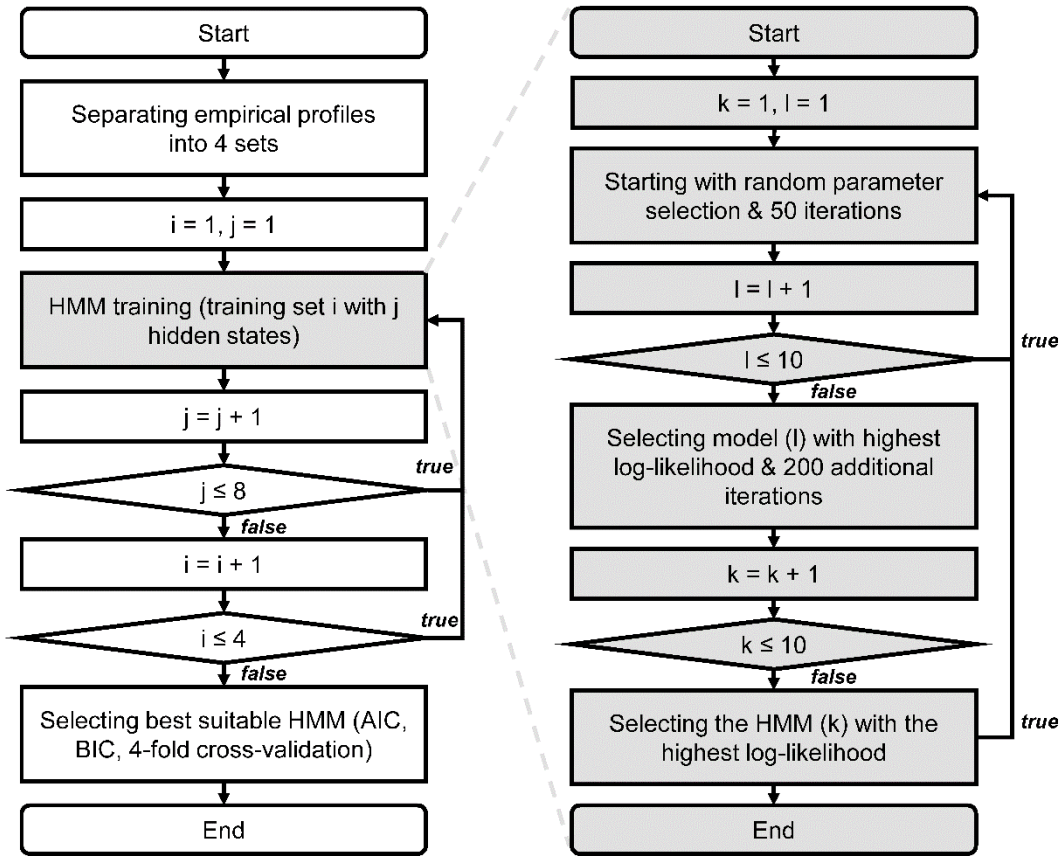
Fig A.1 *Implementation strategy of the Baum Welch algorithm in the case study (based on Biernacki et al. [59])*
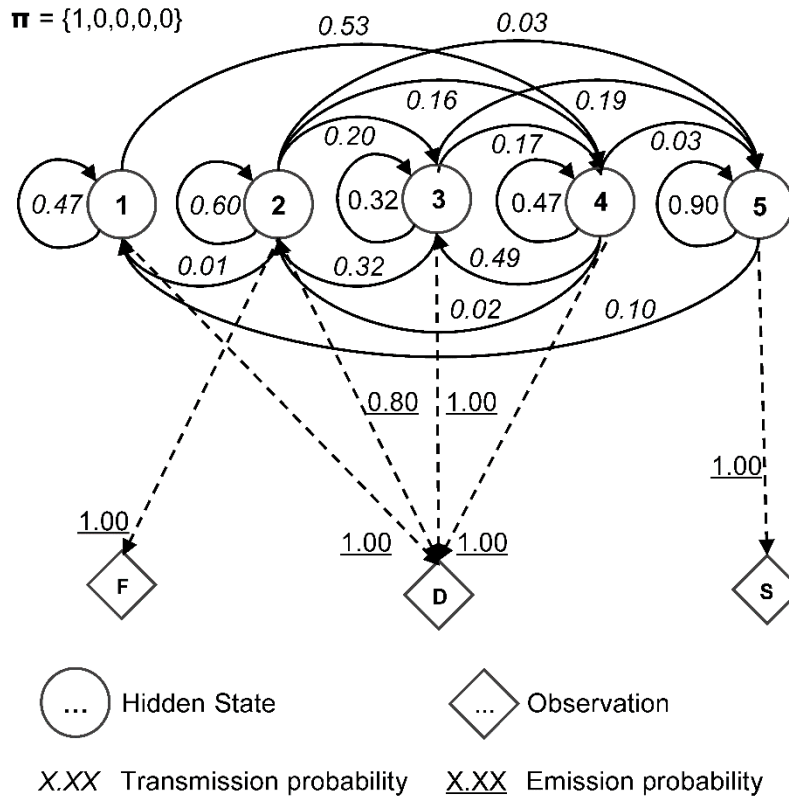

Fig. A.2 *The relationship of hidden states and observations in the multinomial HMM (case study example)*

Appendix B
Fast Forward Selection (FFS) heuristic

The fast forward selection (FFS) heuristic stepwise selects the scenario from the set of unselected scenarios that has the shortest (updated) Kantorovich distance to the remaining scenarios and is, therefore, the most representative one. The distance between the scenarios is measured with $c(\omega_i, \omega_j)$ which is the sum of a norm of all the distances at any point t in T between the scenarios. The Euclidean norm is used to measure the distance. N is the target number of scenarios. FFS proceeds as follows:

- Step 1:

  The distance $c_{kj}^{[1]} := c(\omega_k, \omega_j)$ between all scenario pairs $k, j = 1, \dots, N$ is calculated.

  The weighted distance $z_l^{[1]} := \sum_{j \neq l} p_j c_{jl}^{[1]}$ of each scenario $l = 1, \dots, N$ to the rest is computed.

  Scenario $s_1 = \arg \min_{l=1,\dots,N} z_l^{[1]}$ is selected and $J^{[1]} = 1, \dots, N \backslash s_1$ is set.

- Step i:

  1. The scenario pair distance $c_{kj}^{[i]} = \min\left[c_{kj}^{[i-1]}, c_{kj_{i-1}}^{[i-1]}\right]$ is updated for all unselected scenarios $k, j \in J^{[i-1]}$ with the minimum of the original pair distance and the distance to the scenario selected in $i - 1$.

  2. The updated weighted distance $z_l^{[i]} := \sum_{j \in J^{[i-1]} \backslash i} p_j c_{jl}^{[i]}$ of each unselected scenario $l \in J^{[i-1]}$ to the rest is computed.

  3. Scenario $s_i = \arg \min_{l \in J^{[i-1]}} z_l^{[i]}$ is selected and $J^{[i]} = J^{[i-1]} \backslash s_i$ is set.

Step i is repeated until the target number of selected scenarios is reached. To the probability p_j of each selected scenario $j \in J'$ the sum of the probabilities p_i of the unselected scenarios closest to it is added, at the end.

$$q_j = p_j + \sum_{i \in L(j)} p_i , \forall j \in J' \tag{B.1}$$

$$L(j) := \{i \in J \backslash J', j = j(i)\}, \; j(i) = \arg \min_{j \in J'} c_j^{[1]}, i \in J \backslash J' \tag{B.2}$$

Appendix C1
Electric vehicle energy consumption model

The energy consumption is split into three parts: propelling the electric vehicle (EV), additional energy consumption through battery weight, and the auxiliaries' demand.

$$EC^{el}\left(DS_{t,s^{mob}}^{spd}, \boldsymbol{BCAP^G}, Temp_{t,s^{temp}}^{amb}\right) = EC^{prop}\left(DS_{t,s^{mob}}^{spd}\right) + EC^{wght}(\boldsymbol{BCAP^G}) + EC^{aux}\left(Temp_{t,s^{temp}}^{amb}\right) \tag{C.1}$$

A detailed description of forces, resistances, and efficiencies in a dynamic driving model and a discussion of the external influences on energy consumption can be found in the literature [81,87].

Drive cycle	Mean speed
Inner-city (NEDC, phase 1 & WLTP phase 1)	18.5 km/h
Inter-urban (NEDC, phase 2 & WLTP phases 2-4)	63 km/h
Motorway (ADAC BAB)	114 km/h

Table C.1 Drive cycle characteristics of ADAC measurement

The data for the piecewise linear approximation of the energy required for propelling the EV forward is based on real-world measurements taken by the German automobile club ADAC. This study relies on real-world data since the values stated by the manufacturers are measured under laboratory conditions. Different points of measurement are required to

approximate the energy consumption depending on the mean driving speed. Table *c.1* lists the combinations of phases from three driving cycles used by the ADAC for their measurements of inner-city, inter-urban, and motorway consumption [88]. For each of the measurement points the mean speed of different EVs from the mini and small segment was deducted from the applied driving cycles. The force required to overcome the drag resistance is proportional to the square of the speed. To avoid quadratic constraints, it was piecewise linearly approximated by the parameters m_{spd} and b_{spd} (Table C.2).

$$EC^{prop}\left(DS_{t,s^{mob}}^{spd}\right) = m_{spd}DS_{t,s^{mob}}^{spd} + b_{spd} \tag{C.2}$$

$DS_{t,s^{mob}}^{spd}$	(0,18.5]	(18.5,63]	(63, …)
m_{spd}	0	0.5693	1.863
b_{spd}	115.45	104.92	23.43

Table C.2 *Parameters for the piecewise linear approximation of energy consumption for propulsion*

The additional energy required to overcome the increased rolling resistance due to the battery weight is calculated with the energy density ρ^{bat}, the rolling resistance coefficient c_{rr}, and the gravitational constant g.

$$EC^{wght}\left(BCAP^{G}\right) = \frac{BCAP^{G}}{\rho^{bat}}c_{rr}g \tag{C.3}$$

The specific mean energy consumption increases by 0.2524 Wh/km for each additional kWh of capacity, which fits the around 3% increase per 100 kg additional weight [89]. Higher weight also increases the vehicle inertia which leads to higher losses in recuperation. This is neglected in this study since the increases are small and difficult to assess.

The specific energy consumption of the auxiliaries is highly sensitive to the speed of the EV $DS_{t,s^{mob}}^{spd}$ since the power demand of the auxiliaries is assumed to be constant. At a constant load, the specific energy consumption increases at a slower speed. For the auxiliaries, a baseload of 500 W is set. This value is based on empiric measurements and literature values [81]. The specific energy consumption is piecewise linearly approximated by five separate functions (Table C.3).

$$EC^{aux}\left(DS_{t,s^{mob}}^{spd}, Temp_{t,s^{temp}}^{amb}\right) = \left(m_{temp}DS_{t,s^{mob}}^{spd} + b_{temp}\right)f_{temp}\left(Temp_{t,s^{temp}}^{amb}\right) \tag{C.4}$$

$DS_{t,s^{mob}}^{spd}$	(0,5]	(5,10]	(10,20]	(20,40]	(40, …)
m_{temp}	-40	-10	-2.5	-0.625	-5/48
b_{temp}	300	150	75	37.5	50/3

Table C.3 *Parameters for the piecewise linear approximation energy consumption of the auxiliaries*

Heating and cooling the passenger cabin requires additional power. In this study four levels of additional power demand factor f_{temp} to heat or cool the cabin are set depending on the ambient temperature (Table C.4). Other temperature dependencies such as increased losses due to higher battery inner-resistance or lower recuperation power are neglected in this study. Therefore, the ambient temperature from the temperature scenarios $Temp_{t,s^{temp}}^{amb}$ is taken as variable input to the energy consumption function.

$Temp_{t,s^{temp}}^{amb}$	(…,0)	[0,10)	[10,15)	[15,25)	[25,30)	[30, …)
f_{temp}	4	3	2	1	2	3

Table C.4 *Factor for the auxiliaries' intensity of use dependent on the outside temperature*

Appendix C2
Electric vehicle charging load-curves
The input data for the charging curves comes from own empirical measurements (IIP database). The maximum charging power P_c^{maxcrg} and the reduction points RP_c for different EVs for single-phased 2.2 kW and 3.7 kW charging were recorded with an external energy measurement device directly at the power outlet. The three-phased 11 kW (16 A, 400 V) and 22 kW (32 A, 400 V) charging curves were taken from the EV battery management system data. Hence, the charging losses in the on-board charging unit must be considered when calculating their maximum power at the grid level. The recorded curves are validated by other empirical results from the literature [56]. Due to the modeling choice of the flexible battery capacity, the linear increase in charging power as a result of the increase in battery voltage at a constant current level had to be neglected.

Appendix D1

s^{mob}		5		10		15		20		25	
	c	z_s^{mob*}	$BCAP^G$	z_s^{mob*}	$BCAP^G$	z_s^{mob*}	$BCAP^G$	z_s^{mob*}	$BCAP^G$	z_s^{mob*}	$BCAP^G$
FFS	2.2	13,392	18	13,460	18	16,721	44	18,220	56	18,237	56
	3.7	13,931	18	13,999	18	16,389	37	18,511	54	18,527	54
	11	14,471	18	14,539	18	16,929	37	18,055	46	18,071	46
	22	15,011	18	15,078	18	17,468	37	18,470	45	18,486	45
FSWC_S	2.2	17,252	47	18,281	52	19,360	60	19,383	60	19,390	60
	3.7	17,169	42	18,446	49	19,650	58	19,673	58	19,680	58
	11	17,459	40	18.361	44	18,816	47	18,839	47	18,846	47
	22	17,999	40	18,901	44	19,106	45	19,128	45	19,136	45
FSWC_O	2.2	20,149	44	21,227	52	22,193	60	22,192	60	22,222	60
	3.7	20,309	41	21,513	50	22,479	58	22,478	58	22,508	58
	11	19,710	32	21,673	47	21,627	47	21,626	47	21,656	47
	22	19,997	30	21,580	42	21,913	45	21,912	45	21,942	45

Table D.1 Optimal values and battery capacities for the three scenario reduction heuristics and four different charging capacities (the cost-minimal decision set for each subset size is highlighted; FFS with $s^{temp} = 10$)

Appendix D2

s^{temp}		5		10		15		20	
	c [kW]	z_s^{mob*}	$BCAP^G$	z_s^{mob*}	$BCAP^G$	z_s^{mob*}	$BCAP^G$	z_s^{mob*}	$BCAP^G$
FFS	2.2	22,060	59	22,192	60	22,193	60	22,193	60
	3.7	22,346	57	22,479	58	22,479	58	22,479	58
	11	21,620	47	21,626	47	21,627	47	21,627	47
	22	21,907	45	21,913	45	21,913	45	21,913	45

Table D.2 Optimal values and battery capacities for the FFS scenario reduction heuristic and four different charging capacities (the cost-minimal decision set for each subset size is highlighted; FSWC_O with $s^{mob} = 15$)

Appendix D3

Scenario No.	z_s^{mob*}	$BCAP^G$	c	Probability
37	20,014	33	2.2	0.0200
55	21,863	38	11	0.0008
76	19,520	29	2.2	0.0280
114	15,050	12	2.2	0.1100
238	21,130	28	11	0.0008
542	21,724	35	11	0.0016
774	20,321	44	2.2	0.0012
1004	18,856	25	2.2	0.0568
1036	18,826	22	11	0.0008
1102	23,867	50	2.2	0.0008
1171	21,882	47	11	0.0004
1175	20,677	15	11	0.0012
1214	20,241	18	11	0.0016
1310	20,441	34	2.2	0.0100
1404	16,710	16	2.2	0.1920
1439	14,140	9	2.2	0.1084
1497	17,328	21	2.2	0.1452
1593	21,370	40	2.2	0.0028
1627	18,143	23	2.2	0.0912
1763	26,263	54	11	0.0004
1867	15,854	16	2.2	0.2116
1928	21,395	37	2.2	0.0044
1978	19,745	20	3.7	0.0028
2019	12,719	6	2.2	0.0068
2393	23,490	29	2.2	0.0004
		Cumulative probability of scenarios with 2.2 kW		0.9896
		Cumulative probability of scenarios with 3.7 kW		0.0028
		Cumulative probability of scenarios with 11 kW		0.0076
		Cumulative probability of scenarios with ≤ 30 kWh		0.9576
		Cumulative probability of scenarios with ≤ 40 kWh		0.9972

Table D.3 Optimal solutions for the individual mobility scenarios and the associated probabilities for the SAA (FSWC_O with $s^{mob} = 15$, FFS with $s^{temp} = 10$)

References

[1]   European Commission. A European Strategy for Low-Emission Mobility 2016. https://ec.europa.eu/clima/policies/transport_en (accessed December 26, 2017).

[2]   Jochem P, Doll C, Fichtner W. External costs of electric vehicles. Transp Res Part D Transp Environ 2016;42:60–76. https://doi.org/10.1016/j.trd.2015.09.022.

[3]   Creutzig F, Jochem P, Edelenbosch OY, Mattauch L, van Vuuren DP, McCollum D, et al. Energy and environment. Transport: A roadblock to climate change mitigation? Science 2015;350:911–2. https://doi.org/10.1126/science.aac8033.

[4]   Ketelaer T, Kaschub T, Jochem P, Fichtner W. The potential of carbon dioxide emission reductions in German commercial transport by electric vehicles. Int J Environ Sci Technol 2014. https://doi.org/10.1007/s13762-014-0631-y.

[5]   Gnann T, Plötz P, Kühn A, Wietschel M. Modelling market diffusion of electric vehicles with real world driving data - German market and policy options. Transp Res Part A Policy Pract 2015;77:95–112. https://doi.org/10.1016/j.tra.2015.04.001.

[6]   Plötz P, Gnann T, Kuehn A, Wietschel M. Markthochlaufszenarien für Elektrofahrzeuge (Langfassung). Karlsruhe: 2013.

[7]   Nesbitt K, Sperling D. Fleet purchase behavior: decision processes and implications for new vehicle technologies and fuels. Transp Res Part C 2001;9:297–318.

[8]   KBA. Monatliche Neuzulassungen. Neuzulassungen von Pers Nach Marken Und Model 2017. http://www.kba.de/DE/Statistik/Fahrzeuge/Neuzulassungen/MonatlicheNeuzulassungen/monatl _neuzulassungen_node.html.

[9]   Liu K, Wang J, Yamamoto T, Morikawa T. Exploring the interactive e ff ects of ambient temperature and vehicle auxiliary loads on electric vehicle energy consumption. Appl Energy 2017:0–1. https://doi.org/10.1016/j.apenergy.2017.08.074.

[10]   Neubauer J, Wood E. Thru-life impacts of driver aggression, climate, cabin thermal management, and battery thermal management on battery electric vehicle utility. J Power Sources 2014;259:262–75. https://doi.org/10.1016/j.jpowsour.2014.02.083.

[11]   Schücking M, Jochem P, Fichtner W, Wollersheim O, Stella K. Influencing factors on specific energy consumption of EV in extensive operations. EVS 2016 - 29th Int. Electr. Veh. Symp., 2016.

[12]   Statistisches Bundesamt. Pflegestatistik 2015. 2017.

[13]   de Souza Dutra MD, Anjos MF, Le Digabel S. A general framework for customized transition to smart homes. Energy 2019;189. https://doi.org/https://doi.org/10.1016/j.energy.2019.116138.

[14]   Kaschub T, Jochem P, Fichtner W. Solar energy storage in German households: profitability, load changes and flexibility. Energy Policy 2016;98:520–32. https://doi.org/https://doi.org/10.1016/j.enpol.2016.09.017.

[15]   Hiermann G, Puchinger J, Ropke S, Hartl RF. The Electric Fleet Size and Mix Vehicle Routing Problem with Time Windows and Recharging Stations. Eur J Oper Res 2016;252:995–1018. https://doi.org/10.1016/j.ejor.2016.01.038.

[16]   Davis BA, Figliozzi MA. A methodology to evaluate the competitiveness of electric delivery trucks. Transp Res Part E Logist Transp Rev 2013;49:8–23. https://doi.org/10.1016/j.tre.2012.07.003.

[17]   Kuppusamy S, Magazine MJ, Rao U. Electric vehicle adoption decisions in a fleet environment. Eur J Oper Res 2017;262:123–35. https://doi.org/10.1016/j.ejor.2017.03.039.

[18]   Lebeau P, De Cauwer C, Van Mierlo J, Macharis C, Verbeke W, Coosemans T. Conventional, Hybrid, or Electric Vehicles: Which Technology for an Urban Distribution Centre? Sci World J 2015;2015. https://doi.org/10.1155/2015/302867.

[19]   Sathaye N. The optimal design and cost implications of electric vehicle taxi systems. Transp Res Part B Methodol 2014;67:264–83. https://doi.org/10.1016/j.trb.2014.05.009.

[20]   Iversen EB, Morales JM, Madsen H. Optimal charging of an electric vehicle using a Markov decision process. Appl Energy 2014;123:1–12. https://doi.org/10.1016/j.apenergy.2014.02.003.

[21]   Škugor B, Deur J. Dynamic programming-based optimisation of charging an electric vehicle fleet system represented by an aggregate battery model. Energy 2015;92:456–65. https://doi.org/10.1016/j.energy.2015.03.057.

[22]   Škugor B, Deur J. A novel model of electric vehicle fleet aggregate battery for energy planning studies. Energy 2015;92:444–55. https://doi.org/10.1016/j.energy.2015.05.030.

[23]   Wu X, Hu X, Moura S, Yin X, Pickert V. Stochastic control of smart home energy management with plug-in electric vehicle battery energy storage and photovoltaic array. J Power Sources 2016;333:203–12. https://doi.org/10.1016/j.jpowsour.2016.09.157.

[24]   Kley F. Ladeinfrastrukturen für Elektrofahrzeuge. Karlsruhe: Fraunhofer Verlag; 2011.

[25]   Birge JR, Louveaux F. Introduction to Stochastic Programming. 2nd ed. New York: Springer; 2011. https://doi.org/10.1007/978-1-4614-0237-4.

[26]   Wallace SW, Ziemba WT. Applications of Stochastic Programming. SIAM; 2005.

[27]   Di Domenica N, Lucas C, Mitra G, Valente P. Scenario generation for stochastic programming and simulation: A modelling perspective. IMA J Manag Math 2009;20:1–38. https://doi.org/10.1093/imaman/dpm027.

[28]   Long Y, Lee LH, Chew EP. The sample average approximation method for empty container repositioning with uncertainties. Eur J Oper Res 2012;222:65–75. https://doi.org/10.1016/j.ejor.2012.04.018.

[29]   Shapiro A. Sample Average Approximation. In: Gass SI, Fu MC, editors. Encycl. Oper. Res. Manag. Sci., Springer, Boston, MA; 2013. https://doi.org/10.1007/978-1-4419-1153-7.

[30]   Heitsch H, Römisch W. Scenario Reduction Algorithms in Stochastic Programming. Comput Optim Appl 2003;24:187–206. https://doi.org/https://doi.org/10.1023/A:1021805924152.

[31]   Lin Z, Dong J, Liu C, Greene DL. PHEV Energy Use Estimation : Validating the Gamma Distribution for Representing the Random Daily Driving Distance. Transp. Res. Board 2012 Annu. Meet., 2012.

[32]   Khoo YB, Wang C-H, Paevere P, Higgins A. Statistical modeling of Electric Vehicle electricity consumption in the Victorian EV Trial, Australia. Transp Res Part D Transp Environ 2014;32:263–77. https://doi.org/10.1016/j.trd.2014.08.017.

[33]   Plötz P, Jakobsson N, Sprei F, Karlsson S. On the distribution of individual daily vehicle driving distances. Eur. Electr. Veh. Congr. Brussels, Belgium, 3rd – 5th December 2014, Brussels, Belgium: 2014, p. 1–9.

[34]   Shi S, Lin N, Zhang Y, Cheng J, Huang C, Liu L, et al. Research on Markov property analysis of driving cycles and its application. Transp Res Part D Transp Environ 2016;47:171–81. https://doi.org/10.1016/j.trd.2016.05.013.

[35]   Ashtari A, Bibeau E, Shahidinejad S. Using Large Driving Record Samples and a Stochastic Approach for Real-World Driving Cycle Construction: Winnipeg Driving Cycle. Transp Sci 2014;48:170–83. https://doi.org/10.1287/trsc.1120.0447.

[36]   Zhang J, Wang Z, Liu P, Zhang Z, Li X, Qu C. Driving cycles construction for electric vehicles considering road environment : A case study in Beijing. Appl Energy 2019;253. https://doi.org/https://doi.org/10.1016/j.apenergy.2019.113514.

[37]   Jiang P, Liu X, Zhang J, Yuan X. A framework based on hidden Markov model with adaptive weighting for microcystin forecasting and early-warning. Decis Support Syst 2016;84:89–103. https://doi.org/10.1016/j.dss.2016.02.003.

[38]   Yumei L, Anderson-Sprecher R. Hidden Markov Modeling of Waiting Times in the 1985 Yellowstone Earthquake Swarm. Pure Appl Geophys 2013;170:785–95. https://doi.org/10.1007/s00024-011-0323-1.

[39]   Dias JG, Vermunt JK, Ramos S. Clustering financial time series: New insights from an extended hidden Markov model. Eur J Oper Res 2015;243:852–64. https://doi.org/10.1016/j.ejor.2014.12.041.

[40]   Giampietro M, Guidolin M, Pedio M. Estimating stochastic discount factor models with hidden

regimes: Applications to commodity pricing. Eur J Oper Res 2018;265:685–702. https://doi.org/10.1016/j.ejor.2017.07.045.

[41]   Kim MJ, Jiang R, Makis V, Lee CG. Optimal Bayesian fault prediction scheme for a partially observable system subject to random failure. Eur J Oper Res 2011;214:331–9. https://doi.org/10.1016/j.ejor.2011.04.023.

[42]   Zhou ZJ, Hu CH, Xu DL, Chen MY, Zhou DH. A model for real-time failure prognosis based on hidden Markov model and belief rule base. Eur J Oper Res 2010;207:269–83. https://doi.org/10.1016/j.ejor.2010.03.032.

[43]   Jiang P, Liu X. Hidden Markov model for municipal waste generation forecasting under uncertainties. Eur J Oper Res 2016;250:639–51. https://doi.org/10.1016/j.ejor.2015.09.018.

[44]   Zucchini W, MacDonald IL, Langrock R. Hidden Markov Models for Time Series - An Introduction Using R. 2nd ed. Boca Raton, Florida: CRC Press Taylor & Francis Group; 2016.

[45]   Iversen EB, Møller JK, Morales JM, Madsen H. Inhomogeneous Markov Models for Describing Driving Patterns. IEEE Trans Power Syst 2017;8:581–8. https://doi.org/10.1109/TSG.2016.2520661.

[46]   Milburn AB. Operations Research Applications in Home Healthcare. In: Hillier FS, editor. Handb. Healthc. Syst. Sched., New York: Springer; 2012, p. 281–302. https://doi.org/10.1007/978-1-4614-1734-7.

[47]   Yavuz M, Çapar İ. Alternative-Fuel Vehicle Adoption in Service Fleets: Impact Evaluation Through Optimization Modeling. Transp Sci 2017;51:480–93. https://doi.org/10.1287/trsc.2016.0697.

[48]   Ellram LM. An analysis approach for purchasing. Int J Phys Distrib Logist Manag 1995;25:4–23. https://doi.org/https://doi.org/10.1108/02635571111118305.

[49]   Götze U, Weber T. ZP-Stichwort : Total Cost of Ownership. Zeitschrift Für Plan Unternehmenssteuerung 2008;19:249–57. https://doi.org/10.1007/s00187-008-0054-3.

[50]   Linz S, Dexheimer V, Kathe A. Hedonische Preismessung bei Gebrauchtwagen. Wirtsch Stat 2003.

[51]   Fischhaber S, Regett A, Schuster SF, Hesse DH. Second-Life-Konzepte für Lithium-Ionen-Batterien aus Elektrofahrzeugen. Frankfurt, Germany: 2016.

[52]   Mallia E, Finley D, Bauman J, Goody M. Using EV Telematics to Monitor Real-World Battery Health for EV Owners and Fleet Operators. EVS 2016 - 29th Int. Electr. Veh. Symp., 2016, p. 1–11.

[53]   Marongiu A, Roscher M, Sauer DU. Influence of the vehicle-to-grid strategy on the aging behavior of lithium battery electric vehicles. Appl Energy 2015;137:899–912. https://doi.org/10.1016/j.apenergy.2014.06.063.

[54]   Montoya A, Guéret C, Mendoza JE, Villegas JG. The electric vehicle routing problem with nonlinear charging function. Transp Res Part B Methodol 2017;103:87–110. https://doi.org/10.1016/j.trb.2017.02.004.

[55]   Schücking M, Jochem P, Fichtner W, Wollersheim O, Stella K. Charging strategies for economic operations of electric vehicles in commercial applications. Transp Res Part D Transp Environ 2017;51. https://doi.org/10.1016/j.trd.2016.11.032.

[56]   Landau M, Prior J, Gaber R, Scheibe M, Marklein R, Kirchhof J. Technische Begleitforschung Allianz Elektromobilität - TeBALE Abschlussbericht. Kassel, Germany: 2017.

[57]   Apostolaki-Iosifidou E, Codani P, Kempton W. Measurement of power loss during electric vehicle charging and discharging. Energy 2017;127:730–42.

https://doi.org/10.1016/j.energy.2017.03.015.

[58] Baum LE, Petrie T, Soules G, Weiss N. A Maximization Technique Occurring in the Statistical Analysis of Probabilistic Functions of Markov Chains. Ann Math Stat 1970;41:164–71.

[59] Biernacki C, Celeux G, Govaert G. Choosing starting values for the EM algorithm for getting the highest likelihood in multivariate Gaussian mixture models. Comput Stat Data Anal 2003;41:561–75. https://doi.org/https://doi.org/10.1016/S0167-9473(02)00163-9.

[60] Karlis D, Xekalaki E. Choosing initial values for the EM algorithm for finite mixtures. Comput Stat 2003;41:577–90. https://doi.org/10.1016/S0167-9473(02)00177-9.

[61] Akaike H. A New Look at the Statistical Model Identification. IEEE Trans Automat Contr 1974;19:716–23. https://doi.org/10.1109/TAC.1974.1100705.

[62] Schwarz G. Estimating the Dimension of a Model. Ann Stat 1978;6:461–4.

[63] Smyth P. Model selection for probabilistic clustering using cross-validated likelihood. Stat Comput 2000;10:63–72. https://doi.org/https://doi.org/10.1023/A:1008940618127.

[64] Celeux G, Durand J-B. Selecting hidden Markov model state number with cross-validated likelihood. Comput Stat 2008;23:541–64. https://doi.org/10.1007/s00180-007-0097-1.

[65] Lee TK, Bareket Z, Gordon T, Filipi ZS. Stochastic modeling for studies of real-world PHEV usage: Driving schedule and daily temporal distributions. IEEE Trans Veh Technol 2012;61:1493–502. https://doi.org/10.1109/TVT.2011.2181191.

[66] Dupačová J, Gröwe-Kuska N, Römisch W. Scenario reduction in stochastic programming. Math Program 2003;95:493–511. https://doi.org/https://doi.org/10.1007/s10107-002-0331-0.

[67] Feng Y, Ryan S. Scenario construction and reduction applied to stochastic power generation expansion planning. Comput Oper Res 2013;40:9–23. https://doi.org/10.1016/j.cor.2012.05.005.

[68] Morales JM, Pineda S, Conejo AJ, Carrión M. Scenario reduction for futures market trading in electricity markets. IEEE Trans Power Syst 2009;24:878–88. https://doi.org/10.1109/TPWRS.2009.2016072.

[69] Papavasiliou A, Oren SS. Multiarea Stochastic Unit Commitment for High Wind Penetration in a Transmission Constrained Network. Oper Res 2013;61:578–92. https://doi.org/10.1287/opre.2013.1174.

[70] Lloyd SP. Least Squares Quantization in PCM. IEEE Trans Inf Theory 1982;28:129–37. https://doi.org/10.1109/TIT.1982.1056489.

[71] Arthur D, Vassilvitskii S. K-Means++: The Advantages of Careful Seeding. Proc. Eighteenth Annu. ACM-SIAM Symp. Discret. Algorithms, New Orleans, Louisiana, USA: 2007, p. 1027–35. https://doi.org/10.1145/1283383.1283494.

[72] Faria R, Marques P, Moura P, Freire F, Delgado J, de Almeida AT. Impact of the electricity mix and use profile in the life-cycle assessment of electric vehicles. Renew Sustain Energy Rev 2013;24:271–87. https://doi.org/10.1016/j.rser.2013.03.063.

[73] Greaves S, Backman H, Ellison AB. An empirical assessment of the feasibility of battery electric vehicles for day-to-day driving. Transp Res Part A Policy Pract 2014;66:226–37. https://doi.org/10.1016/j.tra.2014.05.011.

[74] Wu X, Freese D, Cabrera A, Kitch WA. Electric Vehicles ' Energy Consumption Measurement and Estimation. Transp Res Part D Transp Environ 2015;34:52–67. https://doi.org/10.1016/j.trd.2014.10.007.

[75] ADAC. Vehicle database 2017.

https://www.adac.de/infotestrat/autodatenbank/autokatalog/default.aspx (accessed November 17, 2017).

[76] McKinsey. Electrifying insights: How automakers can drive electrified vehicle sales and profitability. 2017.

[77] Nykvist B, Nilsson M. Rapidly falling costs of battery packs for electric vehicles. Nat Clim Chang 2015;5:329–32. https://doi.org/10.1038/nclimate2564.

[78] Chediak M. The Latest Bull Case for Electric Cars: the Cheapest Batteries Ever. Bloom New Energy Financ 2017.

[79] KPMG. Kapitalkostenstudie 2016. 2016.

[80] Bickert S, Kampker A, Greger D. Developments of CO_2 -emissions and costs for small electric and combustion engine vehicles in Germany. Transp Res Part D Transp Environ 2015;36:138–51.

[81] Linssen J, Schulz A, Mischinger S, Maas H, Weinmann O, Abbasi E, et al. Netzintegration von Fahrzeugen mit elektrifizierten Antriebssystemen in bestehende und zukünftige Energieversorgungsstrukturen. Juelich: Forschungszentrum Jülich GmbH Zentralbibliothek, Verlag; 2012.

[82] Richter J, Lindenberger D. Potentiale der Elektromobilität bis 2050. Köln: 2010.

[83] REM2030. Codebook data source: REM2030 data 2015.

[84] DWD. Historical hourly station observations of 2m air temperature and humidity for Germany - Version v005 2017.

[85] Graham C, Talay D. Stochastic Simulation and Monte Carlo Methods. vol. 68. Berlin, Germany: Springer; 2013. https://doi.org/10.1007/978-3-642-39363-1.

[86] Dempster AAP, Laird NM, Rubin DB. Maximum Likelihood from Incomplete Data via the EM Algorithm. J R Stat Soc Ser B 1977;39:1–38.

[87] Gerssen-Gondelach SJ, Faaij APC. Performance of batteries for electric vehicles on short and longer term. J Power Sources 2012;212:111–29. https://doi.org/10.1016/j.jpowsour.2012.03.085.

[88] ADAC. EcoTest - Test- und Bewertungskriterien (2012-16). 2016.

[89] Van Vliet O, Brouwer AS, Kuramochi T, Van Den Broek M, Faaij A. Energy use, cost and CO2 emissions of electric cars. J Power Sources 2011;196:2298–310. https://doi.org/10.1016/j.jpowsour.2010.09.119.

Working Paper Series in Production and Energy

www.iip.kit.edu